2013

Effect of the Brownstone Moisture Content at Application Time of a Water Repellent Treatment

Yun Liu
University of Pennsylvania

Effect of the Brownstone Moisture Content at Application Time of a Water Repellent Treatment

Abstract
Portland brownstone is a widely used building material that is susceptible to severe deterioration from weathering. This type of stone contains expansive clay minerals that may cause damage during wetting/drying cycles. Water repellent treatments could, in principle, reduce this problem. The study presents results obtained from water vapor transmission tests, sorption isotherms, and hygric linear expansion of Portland brownstone treated with two types of water repellent, water based Siloxane PD and solvent based Natural Stone. The treatments were applied at two different moisture contents of the stone samples. The results obtained from the various tests showed no significant differences between the treated and control samples by overall statistical data analysis. The water based water repellent treated samples showed that those treated at lower moisture content adsorbed less moisture than those conditioned at higher one, and furthermore, they appeared to adsorb less moisture than the controls. Also the hygroscopic swelling showed no significant difference with the controls. However, the hygroscopic swelling of the sandstone was significantly modified by the solvent based water repellent. This water repellent had the opposite behavior to that of the water based one, the samples treated at a lower moisture content adsorbed more moisture than those treated at a higher one.

Keywords
sandstone, hydrophobization, moisture adsorption, hygric expansion, statistical analysis

Disciplines
Historic Preservation and Conservation

Comments
Suggested Citation:

Liu, Yun (2013). *Effect of the Brownstone Moisture Content at Application Time of a Water Repellent Treatment*. (Masters Thesis). University of Pennsylvania, Philadelphia, PA.

EFFECT OF THE BROWNSTONE MOISTURE CONTENT AT APPLICATION TIME OF A WATER REPELLENT TREATMENT

Yun Liu

A THESIS

in

Historic Preservation

Presented to the Faculties of the University of Pennsylvania in Partial Fulfillment of the Requirements of the Degree of

MASTER OF SCIENCE IN HISTORIC PRESERVATION

2013

_____

Advisor

A. Elena Charola, Ph.D.

Lecturer in Historic Preservation

_____

Program Chair

Randall F. Mason, Ph.D.

Associate Professor

Acknowledgements

I would like to thank the following individuals for their assistance with the thesis in all respects. Mike Meehen of the Portland Brownstone Quarries, Jason Burnitskie and Gino Varacalli of Dan Lepore & Sons Company, Jessica Fotch, Kalen D. McNabb and Dennis Pierattini of the University of Pennsylvania generously offered help with the preparation of the testing materials. John Walsh, Steven T. Szewczyk, and Dr. T. Jamie Ford kindly assisted with instrumental analysis.

I wish to thank the faculty of the Historic Preservation program, especially Dr. Randall F. Mason, Prof. Frank G. Matero, and Dr. Aaron V. Wunsch, for their intelligence and enduring support in every respect of the graduate study. Thanks also to my classmates for companionship, sharing, and encouragement.

My special thanks go to Victoria Pingarron Alvarez, the manager of Architectural Conservation Laboratory at PennDesign, for her continuing effort in creating an organized space for experiments and conversations.

My deepest appreciation goes to Dr. A. Elena Charola, my thesis advisor, who saw me through the whole project, provided instructions, talked things over, assisted with the experiments and data analysis, read, wrote, and offered comments. Her constant support never failed even in times of disappointment.

My greatest debt is to my parents, for being my anchor, and always putting up with me and all of my nervousness.

I am grateful to all those who have been with me over these two years. You made my day in Philly.

Table of Contents

List of Figures

List of Tables

Chapter 1 Introduction

Overview of the Problem

Water is either the cause or an accelerating factor for most of the deterioration affecting stone. It contributes to various deterioration mechanisms such as transport and crystallization of soluble salts, freeze-thaw and bio-colonization among others. All of these processes require the presence of water.

There is a long tradition in the use of water repellent agents to prevent liquid water ingress so as to prolong the service life of masonry structures. The hydrophobization treatments provide protection to stone surfaces, but many variables can affect their performance (Charola 2001; Charola 1995). The studies of these variables have mostly focused on the type of substrate, the active ingredient concentration, and the nature of the polymerization reactions. Although it is well known that these reactions are influenced by the conditions under which they occur, such as temperature and relative humidity of the environment, seldom have these issues been studied in detail.

Recently, research conducted at the Swedish Cement and Concrete Research Institute showed that the moisture content of concrete at the time of application of the water repellent affects the amount of hygroscopic moisture the treated concrete is capable of taking up subsequently (Johansson et al. 2008). The study also

provided information regarding what part of the pore system is actually treated, and how the treatment affects the penetration depth of the water repellent. Based on it, this thesis investigates whether natural stones show the same behavior as concrete upon application of a water repellent, as in the case of concrete the moisture adsorption could be related to the final setting reactions, i.e., hydrolysis of the cement.

For this purpose, the fine-grained variety of Portland brownstone which has been identified to contain a fair amount of clay and mica was selected for the study (Crosby and Loughlin 1904). This clay-bearing sandstone is highly susceptible to deterioration due to swelling and shrinkage of clay minerals with changes of moisture content, both hygric, in the vapor phase, and hydric, in the liquid water phase (Ruedrich et al. 2010; Jiménez González, Rodríguez Navarro, and Scherer 2008; Wangler and Scherer 2008; Jiménez González, Higgins, and Scherer 2002).

Therefore, this thesis will address two questions:

1. Will the sandstone show the same behavior as concrete regarding the hygroscopic moisture absorption as a function of moisture content at the time of application of the water repellent?

2. Will the water repellent application change the hygroscopic swelling of the sandstones?

The study will evaluate two water repellent agents applied to Portland brownstone conditioned at two relative humidity levels (43% and 75%) at room temperature. The two commercial siloxane based products differ both in the active alkylalkoxysilanes ingredients and in their formulation, one being in a solvent solution and the other in water emulsion, were selected.

The behavior of these products will be based on both the subsequent hygroscopic moisture adsorption (sorption isotherms) and the consequent swelling associated with different moisture contents. Furthermore, the effect these treatments may have on the water vapor permeability of the stone will be determined. The evaluation of the swelling effects is based on linear expansion measurements with a length comparator.

Chapter 2 The Portland Sandstone

2.1 Historical use

Recent studies have clarified that Portland brownstone, as it is known in the market, refers to a sandstone from Early Jurassic period of Portland formation that is found in the Connecticut River Valley and was quarried extensively at Portland, Middlesex County, CT, since the 1640s (Jiménez González, Flatt, and Wangler 2012, 7-8, 73-79; Bell 1985, 31). It was used for dressed foundations and window trims as an easy and cheap substitute for granite or marble (Matero 1982).

In the 1840s, change in taste to Gothic Revival, together with improvements in quarrying methods and transportation, spurred the emergence of the "Brown Decades" in the United States (Matero 1982). Portland brownstone became extensively used for all kinds of building and monumental work in the principal cities along the Atlantic coastline. The 1880 federal census reported that "78.6 percent of New York City buildings employing stone were all or part brownstone, most of which came from Portland."

Changing taste and its rapid deterioration made Portland brownstone unpopular by the end of the 19th century, and all the quarries came to a halt in the 1950s (Bell 1985, 31). In the 1990s a small section of the quarries returned to

operation for conservation projects. Since the land has been put up for sale, the last quarry closed in November 2012.

2.2 Deterioration

Although Portland brownstone is often described as a uniform reddish-brown stone (United States Census Office 10th Census 1883, 127; Bowles 1939, 74; Matero 1982), the quarried stone shows little homogeneity in texture, color, and chemical composition from section to section and from layer to layer (Figure 2.1). This may be one of the reasons why the brownstone was usually placed in the face bedded orientation on buildings to attain a uniform appearance. But the stone exhibits the lowest mechanical resistance to the weight above in this orientation (Jiménez González, Flatt, and Wangler 2012, 40-42), and, on the other hand, water is absorbed most readily in the direction of the lamination by capillarity but goes out slowly across the beddings, which increases the potential of the damage that can result from freeze-thaw, salt crystallization and biocolonization.

Figure 2.1 Photograph of quarry stone showing the heterogeneity from layer to layer.

Early sources define Portland brownstone as durable if carefully selected and properly used, i.e., when laid in the bed, but when it is face bedded, it is generally considered as susceptible to serious deterioration by a range of processes (Bowles 1939, 73-74; Crosby and Loughlin 1904; United States Census Office 10th census 1883, 368). Most of the field-based observations indicate buckling, and eventually contour scaling, as the main damage patterns for this sandstone (Jiménez González,

Flatt, and Wangler 2012, 17-20; Wangler and Scherer 2009, 2007; Snethlage and Wendler 1997). This weathering form has been found related to the damaging stresses generated by swelling, either from clays and/or salt crystallization. The present review will only address the issue of clay swelling.

As summarized by Weiss, three factors can cause swelling in building stones: temperature, moisture, and salts (Weiss et al. 2004). The insensitivity of most sedimentary stones to temperature fluctuation denies its clear-cut causality to weathering (Turkington and Paradise 2005; Weiss et al. 2004). On the other hand, no salts have been reported in the X-ray Diffraction (XRD) analysis for the unweathered Portland brownstone (Jiménez González, Flatt, and Wangler 2012, 35-37). Therefore Portland brownstone can be treated as a salt-free system, in which the swelling can be mainly attributed to the presence of clay minerals that can incorporate water in their structures upon wetting.

2.3 Clay swelling

2.3.1 Introduction

Elemental analysis reveals a high content of alumina in Portland brownstone (United States Census Office 10th Census 1883, 127), which suggests the presence of feldspars and their weathering products, i.e., clays that usually constitute the cementing phase. In fact, as pointed out by Jiménez González et al., the alumina

exists in the form of feldspar and mica rather than clay minerals (Jiménez González, Flatt, and Wangler 2012, 34-35). Extensive analytical studies with XRD analysis, polarized microscopy analysis of thin sections, and Scanning Electron Microscope (SEM) analysis have confirmed that the clay content is below 5 % of the total composition (Jiménez González, Flatt, and Wangler 2012, 37; Wangler and Scherer 2008). Identifiable peaks from XRD analysis of the clays separated from the stone suggest that chlorite is the dominant phyllosilicate mineral with smaller amounts of illite and kaolinite, these are all important clay minerals common present in sedimentary stone, considered as non-expansive with kaolinite being the one that expands least (Wangler and Scherer 2009).

But these non-expansive clay minerals can be swellable in the presence of water when they are stacked on each other in variable amounts and with variable degrees of ordering to form mixed layer clays. All possible combinations of different mineral layers can occur with the changes of pre-existing clay minerals during diagenesis and weathering (Ruedrich et al. 2010; Weaver 1956). Mixed layer clays are commonly present in sedimentary stone and non-expansive chlorite fraction has been found to be randomly distributed through the expansive clay layers (Jiménez González, Flatt, and Wangler 2012, 37).

The presence of expansive clays in Portland brownstone is revealed by polar organic solvent swelling experiments conducted by Wangler and Scherer (2008).

The depressing effect on sample swelling with potassium cations pretreatment and the doubling basal spacing observed upon the sequential addition of methanol and ethylene glycol to the sample correspond to the transition from a monolayer to a bilayer of basal spacing in the theory of the swelling of smectite and vermiculite, both are typical expandable clay minerals in sandstone, including Portland brownstone (Ruedrich et al. 2010; Wangler and Scherer 2008).

These experiments also confirm that intracrystalline swelling is the dominant swelling mechanism in Portland brownstone with little contribution from osmotic effects or capillary pressure (Wangler and Scherer 2008). This swelling is induced by hydration of the interlayer cations, either from expansive or mixed layer clays, which is considered to be a stepwise process from one layer to four layers of water molecules. The hydration is dependent on the type of the clay minerals and the type of counter-ions (Ruedrich et al. 2010; Tambach et al. 2006).

The properties of intracrystalline swelling have been quantitatively studied with experiments and simulations at molecular level using montmorillonite, a typical smectite mineral that yields extreme swelling upon wetting. Water adsorption isotherms and swelling pressure of the system are calculated as a function of the basal spacing at different relative humidity (RH) at which swelling usually occurs (Tambach et al. 2006; Smith 1998; Fu, Zhang, and Low 1990).

Both experiments and molecular computer simulations agree that RH plays a significant role to the magnitude of swelling. Generally, increased RH leads to an increased development of layered hydrates and the corresponding basal spacing (Tambach et al. 2006). This implies that the clay minerals tend to swell more at a higher RH level. At low RH, the tested Na-saturated smectite swells up to about 15Å of basal spacing, whereas at high RH, the swelling increases monotonically and possibly reaches as much as 200Å of basal spacing (Tambach et al. 2006; Tambach, Hensen, and Smit 2004; Fu, Zhang, and Low 1990).

Increased RH also leads to an increased internal pressure normal to the clay platelets. In the case of Wyoming Na-montmorillonite, with controlled basal spacing, pressures generally show the same trend to oscillate above 1 atm at a layer spacing of less than 12 Å and convergence to a subsequent stable state for all RH levels. Nonetheless, higher pressures are always generated with increased RH values (Tambach, Hensen, and Smit 2004).

2.3.2 Hydric swelling

Similar to the research on clay swelling at a micro level, the swelling of stone has been studied by measuring the sorptivity, dimensional expansion, and the generated stresses that are responsible for the damage. As suggested by the mineral studies, if the building stone swells according to the expansive clay minerals, the

sorptivity and the swelling stresses should perform as function of swelling strain with changes of RH.

Most of the studies on the swelling of building stone, including Portland brownstone, have mainly focused on the effect of total immersion in water. The swelling strain is usually measured with a dilatometric method that allows continuous monitoring of the dimensional change of the sample before, during, after immersion in liquid (Wangler and Scherer 2008; Jiménez González and Scherer 2006, 2004; Weiss et al. 2004; Jiménez González, Higgins, and Scherer 2002).

In the case of Portland brownstone, although the expansive clay is in a very small amount (about 0.15% of the total composition) and randomly distributed around chlorite fractions, notable dimensional expansion can still be observed during a wetting cycle (Wangler and Scherer 2008). Due to the stratification, the largest expansion is measured perpendicular to the bedding planes, and a scattering swelling strain ranging from 400 μm/m to 1000 μm/m in this orientation has been reported (Wangler and Scherer 2009).

In general, swelling strain can be one indicator of the damage potential of stone since in principle the resulting movements and displacements from grain to grain within the structure weaken the intergranular bonds, and ultimately destroy the entire grain structure (Snethlage and Wendler 1997). It has also been found that the elastic modulus corresponding to a swelling strain above 1500μm/m typically

exceeds the tensile strength of the stone (Jiménez González, Rodríguez Navarro, and Scherer 2008). But it alone is not sufficient to predict the occurrence of damage. The damaging potential of swelling has been further confirmed by comparing the elastic modulus, viscoelastic relaxation rate with the mechanical properties of the sandstone, such as tensile, shear or compressive strength (Scherer and Jiménez González 2005).

Repeated experiments have shown that both measured and calculated stresses produced during wetting and drying cycles exceeded the strength of Portland brownstone by measuring the warping of thin stone plates (Wangler and Scherer 2009, 2008; Jiménez González and Scherer 2006, 2004; Scherer and Jiménez González 2005; Jiménez González, Higgins, and Scherer 2002). Furthermore, if the wetting of the stone is not uniform, the stresses induced by differential strain can be twice as large as the tensile strength of the stone (Jiménez González, Higgins, and Scherer 2002). Thus the tensile stresses and shear forces developed during drying and wetting may cause cracking and buckling respectively, and eventually result in contour scaling as observed in the field surveys (Jiménez González, Rodríguez Navarro, and Scherer 2008).

Considering the long term effects of swelling, extensive test series are still lacking. One study showed that gradually increased swelling strain has been observed in the case of untreated Portland brownstone from the data collected after

100, 200, and 700 accelerated cycles of wetting and drying with liquid water (Jiménez González and Scherer 2006). This can be attributed to the progressive damage developed with material fatigue that lowers the stiffness to resist the swelling pressure.

2.3.3 Hygric swelling

Only few studies have dealt with the swelling effects of clay minerals in building stone under hygric conditions (Ruedrich et al. 2010; Steindlberger 2004). Swelling properties of eight German sandstones with varying mineralogical compositions have been examined at nine RH stages between 15% and 95% as well as under total immersion. Although large difference exists among different species, a fairly linear increase of water content and swelling strain is observable. A significant change in length, perpendicular to stratification, is mostly observed above 75% RH. The same trend is generally obtained with swelling pressure measurements, but a decrease may be observed at high RH depending on sample species (Ruedrich et al. 2010).

Although hygric swelling is generally less significant as compared to hydric swelling with data obtained in laboratory experiments, unexpected damage may occur with long-term RH changing cycles in field conditions. However more data are in need for the effects of long-term cycles as a function of RH changes.

Chapter 3 Water repellents

3.1 Background of water repellents

The idea of water repellent agents was born with the long tradition of preventing the access of moisture into building stone, which can be traced back to the records from Greek and Roman antiquity. According to Vitruvius and Pliny, oils and waxes were used as a final treatment on the polished marble. These organic substances of natural origin were used to attain water-repellent surfaces on stone materials up to the 1850s, although the purpose of such treatments as hydrorepellent protection measures was seldom addressed specifically (Manaresi 1993).

With the improvements in modern technology, increased concerns of protection and preservation spurred the use of synthetic products such as alkyl siliconates, silanes and siloxanes, as well as perfluoropolyethers in the second half of the 20th century (Charola 1995). Unlike conventional sealants, these water repellent agents stop water drops from entering, but still allow water vapor to pass through. In this way, equilibrium conditions are guaranteed between the interior and the exterior of the treated materials (Charola 2001). Since then, silicone-based water repellent agents developed steadily for commercial use, and have been used

as the most common and effective products to achieve a water repelling effect (Charola 2001; Osterholtz and Pohl 1992).

3.2 Chemistry of silicone-based water repellent agents

Silanes, siloxanes, polysiloxanes, and silicone resins represent the most frequently used groups of organic compounds that form the basis for water repelling systems. All these systems function by penetrating the porous structure of stone through capillarity. But different groups behave differently due to their various molecular sizes associated with different degrees of condensation (van der Klugt and Koek 1995).

Silanes were the name given to the family of compounds that result from silicon and hydrogen links (Si-H). By extension, is has also been applied to those compounds where the Si atom is linked directly to a C atom (Si-C). Silanes used as water repellents are usually linked to one or two alkyl groups the others being alkoxy groups that allow the compound to polymerize and link to the substrate in situ. They have the advantage of good penetration properties due to their low viscosity. But they are very volatile, which may decrease their bonding to the substrate.

The simple silanes polymerize to siloxanes or oligomeric siloxanes (3 to 8 repeating units) and then to polysiloxanes (over 9 repeating units, this being the

average value). They may also cross-link to form silicone resins, which are highly branched siloxanes of higher molecular weight. Si-O-Si bond serves as the backbone of these polymers. Increased polymerization improves the stability and effectiveness of the water repellent treatment but also brings about an increase in viscosity of the products.

3.3 Alkyl-alkoxy-silanes as water repellent agents

Most of the porous inorganic building materials are polar in nature, thus tend to attract water molecules. In principle, alkyl-alkoxy-silanes develop the water repellency by changing the surface properties of the substrate from polar to non-polar, or from hydrophilic to hydrophobic (Charola 2001; Charola 1995). This is accomplished by the presence of the alkyl groups which confer hydrophobicity.

Alkoxy groups serve to polymerize the molecule(s) as well as bond it them to the substrate. The reaction occurs in situ by hydrolysis and condensation. Hydrolyzed alkoxy groups react either with components of the substrate or with one another to form polysiloxanes as final products (Kober 1995; Glowacky et al. 2008; Herb, Brenner-Weiß, and Gerdes 2008; Oehmichen, Gerdes, and Wefer-Roehl 2008). A thorough and detailed explanation of the polymerization from silane, via siloxane, to oligosiloxane or polysiloxane is presented by Arkles (1977). The alkyl groups, on the other hand, function as non-polar tails surrounding the substrate

coated with the siloxane, repelling water molecules away from the surface, thus suppressing the capillary action of water.

Alkyl-alkoxy-silanes are the main active ingredient in the most commonly available water repellent agents that are used to prolong the service life of masonry structures. And in most of them, the alkyl is a methyl ($-CH_3$) group. The low viscosity derived from their low molar masses contributes to their capability to penetrate in depth (Charola, Wheeler, and Freund 1984). In addition, alkyl-alkoxy-silanes are generally safe, stable, and easy to handle. By-products of the hydrolysis reactions are alcohols that are volatile and innocuous to building stone (Lewin and Wheeler 1985)

3.4 Factors that affect their effectiveness

The mechanisms involved in the hydrophobic action are not as yet fully understood. The polymerization and the bonding between the formed polysiloxanes and the substrate, as well as the influence of transport process depend upon the specific conditions existing during the application of the product and of the material treated. Studies suggest that these reactions are influenced by the formulation of the water repellent agents, nature and condition of the substrate, and the environmental conditions, such as temperature and relative humidity, at the moment of application.

3.4.1 Formulation

Since the 1990s, the effectiveness of aqueous dispersions of water repellent agents has been found to be comparable to solvent-based agents in terms of penetration properties, resistance to alkalis, and reduction of capillary water absorption (De Witte et al. 1995; Kober 1995; Charola 2001). Although they may show lower performance under freeze-thaw conditions (Charola 2001), water-based repellent agents can be particularly advantageous in treating moist substrate with a better penetration depth (Biscontin et al. 1995).

The concentration of the active ingredient in the water-based products is critical. Considering the high volatility of silanes, a concentration of more than 40% w/w is recommended as the effective amount for commercial products based on silanes (Charola 1995; De Witte et al. 1995). However, evaporation can take over polymerization with low water content, resulting in lack of deposition and distribution of solid materials (De Witte et al. 1995). The loss due to evaporation prior to hydrolysis and condensation can be as much as 20%-40% (Penati 1993), and it is not compensated by a high reactivity (De Clercq and De Witte 2001a).

Although the alkyl groups do not enter in the polymerization reaction, their length and size influence the hydrophobic performance of the water repellent agents. A comparative study of n-propyltriethoxysilane and iso-octyltriethoxysilane has shown the dependency of the polymerization reaction on the alkyl group in the

silane (Glowacky et al. 2008). Generally, increased length and branching of molecular structure decreases the penetration depth and slows down the reaction (De Clercq and De Witte 2001a). But other studies suggest they can improve the performance of water repellency in terms of long-term effectiveness of the hydrophobization and its resistance to alkaline substrate (Charola 2001; Kober 1995).

3.4.2 Substrate

There is a dependency of the effectiveness of a silicone-based water repellent treatment on the chemical composition of the substrate. The outcome varies among different types of material as well as within the same type of building stone (Charola 2001; Goins et al. 1996; Charola, Wheeler, and Freund 1984). A better result may be achieved in silica containing materials due to their chemical affinity to the reactive alkoxy groups in the agents. But the importance of the substrate varies with different conditions (De Clercq and De Witte 2001a).

Other studies show that porosity of the substrate influences the transport and fixation of moisture and the pore structure seems to play a central role (De Clercq and De Witte 2001a; De Witte et al. 1995). Studies carried out on brick and limestone indicate that a higher number of pores with a diameter between 3.5 and

17 µm, result in an increased effectiveness and durability as tested during artificial aging.

It has been found that the pH value of the substrate largely influences the reaction kinetics of water repellent agents (van der Klugt and Koek 1995; Osterholtz and Pohl 1992). Although variations exist within different active ingredients of the tested agents, both hydrolysis and condensation are proved to be pH dependent with a V-shape curve of which the slowest rate is at approximately pH 6-7.

3.4.3 Environmental conditions

Temperature

Although it is widely known that the chemical reaction is partly restricted by environmental conditions, fewer studies have focused on these issues compared to other factors. One research addressed the reactivity of silanes and siloxanes showing its dependency on the temperature (De Clercq and De Witte 2001b). Generally, all treatments carried out with silicone model compounds on brick and limestone show an excellent water repellent behavior at temperatures within the range between 0°C and 55 °C. An increased reactivity is observed with rising temperature for non-volatile compounds. But shifts may occur with commercial silicone-based water repellents.

Relative Humidity

Porous substrate materials tend to contain a certain amount of physically bound water either through adsorption at lower relative humidities or through capillary condensation at high RH (Johansson et al. 2008). Therefore the RH in the environment will define the moisture content of the substrate structure. Considering that water is one of the reactants in the hydrolysis, which is the first reaction for the eventual polymerization of the water repellent agent, the moisture content of the substrate affects directly the outcome of a water repellent treatment. In addition, the environmental RH sways the evaporation rate of the liquid water repellent agents, which competes with the polymerization reaction.

The dependency of polymerization and evaporation of the liquid monomer of an alkyl-alkoxy-silanes on RH has been studied by visual examination in laboratory settings (Charola, Wheeler, and Freund 1984). In the case of uncatalyzed methyl-trimethoxy-silane polymerizing at different RH with or without substrate, high RH results in high polymerization rate but the polymer does not form a good film because of the subsequent condensation reaction will induce stresses in the polymer. Contrariwise, low RH leads to excessive evaporation with loss of the agent.

With respect to penetration depth, the effect of moisture content inside the substrate at the time of application has been studied by direct measurement as well as by mathematical calculations on various substrates (Johansson et al. 2007; Kober

1995). In general, high moisture content of the substrate at the moment of application leads to a decreased penetration depth of the water repellent agents, resulting in decreased effectiveness subsequently.

The relation between the RH in the environment and the effectiveness of water repellents in terms of moisture transport and fixation has been studied by means of sorption isotherms and liquid water absorption on various substrates. The research conducted on concrete shows that the moisture content of concrete at the time the water repellent is applied affects the amount of water vapor the treated concrete is capable of taking up subsequently (Johansson et al. 2008). The resulting adsorption isotherms deviate largely at high moisture levels, and the deviation starts to occur at about the same RH range at which the concrete had been conditioned when the treatment was applied.

But the influence of the conditioning moisture content seems to be unclear when measured by liquid water absorption (De Clercq and De Witte 2001b). In the research conducted on bricks at different moisture content in a range lower than the critical moisture content, no clear influence of the moisture content of bricks at the time of application on the water absorption properties of the treated samples was observed.

3.5 Negative effects of water repellent agents

Although water repellent agents reduce impact of water in the liquid form, negative effects that the treatments may have on the substrate need to be considered. As summarized by Sasse and Snethlage (1997), hydrophobic treatments may increase the risk of scaling of the building material in the presence of salts and enhance hygric dilatation of the substrate. Uneven decrease of the effectiveness and the possible reduction of water vapor permeability may result in the increase of frost susceptibility (Van Hellemont, De Clercq, and Van Bos 2008). Also, the development of unsightly stripes from biocolonization is a problem (Charola, Delgado Rodrigues, and Vale Anjos 2008). Finally, they may interfere with other conservation treatments (Moreau et al. 2008).

Chapter 4 Methodology

4.1 Overview

The testing program was designed to include the characterization of the Portland brownstone and investigation of its critical properties in the presence of moisture by direct examination of deleterious features, such as clay swelling. For this purpose, both specific tests and measuring equipment were used to assess the effects induced by these features, such as linear expansion.

The characterization of the stone was based on thin section petrography, particle analysis by crushing and sieving the sample, methylene blue absorption, Environmental Scanning Electron Microscope (ESEM) examination coupled with Energy Dispersive Spectroscopy (EDS), and X-ray powder Diffraction (XRD) analysis. These were complemented by water absorption and drying behavior tests.

The effect of the moisture content at the time a water repellent treatment was applied on subsequent moisture adsorption and expansion of the brownstone served as the core experiment. It was supplemented by testing the water vapor transmission and electron microscopy observation of the treated samples, as well as a visual evaluation of the depth of penetration of the water repellents.

All the stone samples used for testing were cut from plates of Portland brownstone purchased from Portland Brownstone Quarries Inc., which was one of

the quarries that served as the main source of the distinctive sandstone during the "Brownstone Era" in the 19th century. Mike Meehan, president and owner of the quarry, opened the quarry in 1993 for restoration projects and closed it by the end of 2012. The quarry was located on the east bank of the Connecticut River at the western edge of the town of Portland, CT. Vertical reddish-brown sandstone cliffs surround deep, tranquil lakes which were created by floods in 1938 (Figure 4.1). Plane-bedded sandstone is the characteristic and dominant type of rock in the quarry. Natural joints, used by quarrymen to divide the brownstone into large blocks are visible in the quarry walls (Figure 4.2).

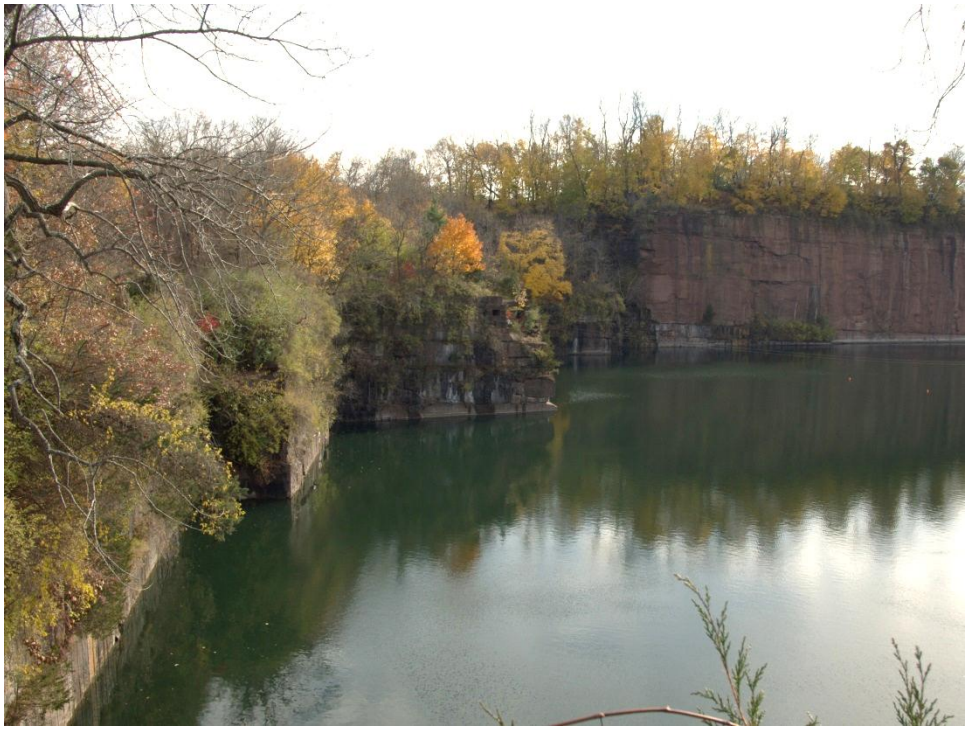

Figure 4.1 Photograph showing the current condition of the Portland brownstone quarries.

Figure 4.2 Photograph showing the bedding and natural joints of the stone in the quarry.

All the tests were conducted according to ASTM (American Society for Testing and Materials), NORMAL (Normativa Manufatti Lapidei, currently accepted as Italian standards UNI), and/or RILEM (Réunion Internationale des Laboratoires et Experts des Matériaux, systèmes de construction et ouvrages) standardized testing methods, as well as literature specifically dealing with the problems that are not included in the standards. The testing methods were modified as necessary in order to best suit the sample conditions, time constraints, and equipment availability. All the tests were conducted in the Architectural Conservation

Laboratory at PennDesign. Temperature in the laboratory was generally maintained at 23 °C with a fluctuation of ±5 °C. The oven temperature was set to 60 °C during all the testing. All the data were recorded and analyzed in metric units.

4.2 Characterization of Portland brownstone

Portland brownstone is formed by sedimentation of discrete particles of various shapes and sizes. The analyses carried out served to characterize not only size and shape of the aggregate, but also its petrographic texture and mineralogical composition as well as assessing the presence of expansive clay minerals.

4.2.1 Particle analysis by sieving

Particle analysis by sieving was conducted in order to characterize and classify the grains of the crushed Portland brownstone by particle size and its distribution. ASTM D422, ASTM D421, and Lab Manual from ICCROM were consulted for the experiment.

Approximately 120 g of Portland brownstone sample was taken from a large bulk sample and crushed in a mortar with a rubber-covered pestle to break down aggregations of particles. Then the sample was oven-dried and weighed until constant weight was attained. Immediately thereafter, the sample was run through a stack of six ASTM standard sieves varying from No. 8 (2.36 mm) to No. 200 (0.075

mm). After shaking by hand for about ten minutes, the weight of material remaining on each sieve as well as that passed the No. 200 sieve was recorded. The weights were summed and compared to the weight obtained before sieving. The test completed when the loss of the retained sample was less than 2 % by weight. The cumulative percentage by weight passing each sieve was calculated in order to draw up a particle size distribution curve in a semi-logarithmic plot.

4.2.2 Methylene blue absorption

The methylene blue absorption is a simple and reliable chemical test to reveal the presence of expansive clay minerals in stone and soil (Stapel and Verhoef 1989; Chiappone et al. 2004). It is based upon the ionic exchange that takes place where the positively charged organic polymeric molecule of methylene blue replaces the exchangeable cations in the clay minerals. The testing method used in this research is called the “spot” method, which is framed with reference to the procedures specified in ASTM C837-09 and the research paper prepared by Stapel and Verhoef (1989).

This test used 0.0094 N (319.9 g/mol) methylene blue solution, which was prepared by dissolving 3.0 g of the oven-dried methylene blue crystals in 250 ml distilled water and diluting to 1 L. The samples were prepared by drying, crushing, and sieving with a standard sieve. About 2.0 g of the sieved particles from No. 16

(1.180 mm) to No. 200 (0.075 mm) as well as those passing No. 200 (<0.075 mm), were used to prepare a suspension in 20 ml distilled water.

The testing set-up is shown in Figure 4.3. Using a 50 ml burette, 0.5 ml methylene blue solution was added to the suspension. After stirring the dispersed mixture for 1 – 2 minutes, a drop of the resulting solution was collected with a glass rod and placed on a Whatman No. 4 filter paper. A dark blue stain was produced with a sharp boundary surrounded by a colorless wet area (Figure 4.4 a). The titration was repeated until a light blue halo was formed around the dark dye spot and persisted for five minutes, which indicated an excess amount of the methylene blue molecule (Figure 4.4 b). The volume of methylene blue solution used was recorded for comparison and further calculations.

Figure 4.3 Methylene blue absorption set-up.

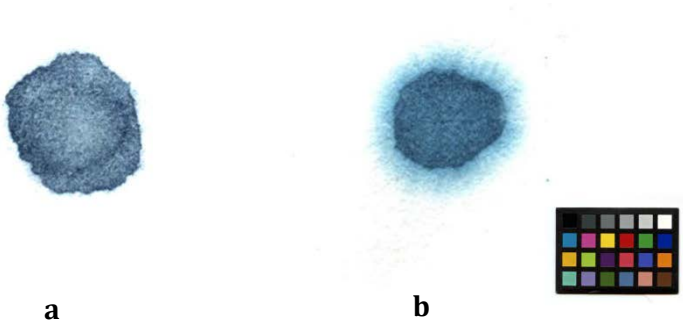

a **b**

Figure 4.4 Examples of methylene blue stains from the test: (a) dark blue dye spot with a sharp boundary; (b) dark blue dye spot with a light blue halo around when there is excessive amount of methylene blue molecule.

4.2.3 X-ray Diffraction (XRD) analysis

The mineralogical composition of the Portland brownstone was determined through X-ray powder Diffraction (XRD) analysis. The observed diffraction peaks can be related to planes of atoms of the minerals present and identified by comparison to standards. An attempt was made to identify the presence of expansive clay minerals using a solvation method (Novich and Martin, 1983). Using glycerol as a solvating agent, distance between parallel planes of atoms of expansive clay minerals increased, which can be observed in a shift of the position of the diffraction peaks.

Two sample slides were prepared using the finer particles below 0.075 mm in size. For the first slide, the powder was dispersed with acetone onto a frosted glass slide to obtain the overall mineralogical composition. An even coating of powder with randomly oriented grains adhered to the glass slide when the solvent evaporated. For the second slide, glycerol was added directly to the particle suspension and mixed thoroughly. About half an hour later, the resultant slurry was packed smoothly on to a frosted glass slide and allowed to dry producing a flat and smooth layer of randomly oriented grains from the maximum possible hydration state. Both sample slides, one at a time, were placed directly into the XRD unit for their analysis.

The XRD spectra were obtained with a Rigaku D/Max-B X-ray diffractometer with Bragg – Brentano parafocusing geometry, a diffracted beam monochromator, and a conventional copper target x-ray tube set to 40 KV and 30 mA. Each sample was analyzed with a 2θ reflection angle from approximately 3 ° to 60 ° at a speed of 2 °/min for about 15 minutes. Data created during analysis was analyzed using the X'Pert HighScore Plus program which matches and identifies the mineralogical composition of the analyzed sample by comparing the peaks present in the sample data with those in a spectral database.

4.2.4 Microscopy

4.2.4.1 Thin-section petrography

Thin-section petrography was used for mineral and texture characterization of Portland brownstone by means of polarized light microscopy. A 30 micron-thick thin-section was prepared across the bedding planes with a clear impregnation resin from a piece of untreated Portland brownstone fragment. It was analyzed petrographically under an Olympus CX31 microscope in cross-polarized transmitted light. Images were taken at 40x, 100x, and 200x magnifications. Features of the sandstone fabric were observed and interpreted in terms of nature of inclusions, matrix textures, pore structures, and the relationship between the clusters of clay minerals and the other mineral grains.

4.2.4.2 Environmental Scanning Electron Microscope analysis

With the aid of an Environmental Scanning Electron Microscope (ESEM), it was possible to examine the morphology of a fracture surface of the Portland brownstone to evaluate the localization of clay particles within the stone matrix, which contributed to a better understanding of the deterioration mechanisms caused by swelling. This technique also enabled to visualize the appearance of the water repellent coatings applied. However, depth of penetration of the two coatings could best be evaluated by spraying a cross section sample with water and measuring the unwetted area.

Freshly exposed sections across the sedimentary bedding planes of both treated and untreated Portland brownstone fractions were examined using the Quanta 600 FEG Mark II environmental scanning electron microscope. Microphotographs of surfaces and inner areas were recorded at 63x, 500x, 1000x and 2000x magnifications. Major and minor elements at desired spots were analyzed semi-quantitatively using a PRINCETON GAMMA TECH (PGT) SPIRIT Instruments energy-dispersive x-ray detector system (EDS) attached to the ESEM.

4.3 Moisture adsorption and linear expansion

The test investigates the dependency of sorption and expansion isotherms of water repellent treated Portland brownstone on the moisture content in the stone at the time the treatment was applied.

A fixed relative humidity (RH) of 43 %, 75 %, and 98 % was established in acrylic desiccator cabinets by setting saturated salt solutions at top and bottom shelves prior to and for the duration of the experiments (Figure 4.5). A fixed RH can be obtained because saturated soluble salt solutions are in equilibrium with a fixed partial vapor pressure of water at constant temperature. Table 4.1 lists the saturated salt solutions that were used for the control of desired humidity conditions in the three desiccators (Young 1967). The RH condition in the desiccators was monitored by Traceable® Humidity-On-A-Card humidity monitor.

Table 4.1 Salts used for the establishment of different RH conditions at 25 °C.

Salt	K_2CO_3	NaCl	$CaSO_4$
RH	43 %	75 %	98-99 %

Figure 4.5 Desiccator of fixed RH established by saturated salt solutions placed in the pans at the bottom and top self of the cabinet.

The water repellent agents used for treatment were PROSOCO Weather Seal Siloxane PD and PROSOCO Weather Seal Natural Stone Treatment with specifications shown in Table 4.2 Both are siloxane based products but differ in solvent, active content concentration, and attached alkyl groups to the backbone polymers.

Table 4.2 Water Repellent Specifications.

WR Type	Solvent	Active Content	Ingredients
Weather Seal Siloxane PD	Water	7 %	methylhydrogen siloxane, alkyl alkoxysilane, ethyl alcohol (hydrolysis by-product)
Weather Seal Natural Stone Treatment	Solvent	11 %	petroleum naphtha, isobutyltriethoxysilane, alkyl polysilicates, ethyl alcohol

The change of length of the samples was measured following ASTM C490 standard. A total of eighteen prisms (25.4 x 25.4 x 127 mm) were cut perpendicular to the sedimentary bedding planes, where the expansion was expected to show the highest value. Two steel gauge studs were fixed to both ends of the prism with J-B Weld epoxy to fit the length comparator. A drawing of the assembly annotated with dimensions is shown in Figure 4.6. The gauge length, which is the nominal length between the innermost ends of the gauge studs, was considered as the true length that was to be measured. However, for the calculations the total length of the setup was adopted since the difference is a determinate error that will not affect the comparison of results. A coding system as shown in Table 4.3 was used for labeling the prisms. Three samples were included in each group in order to be able to randomize the differences in behavior of individual specimens and evaluate the results statistically.

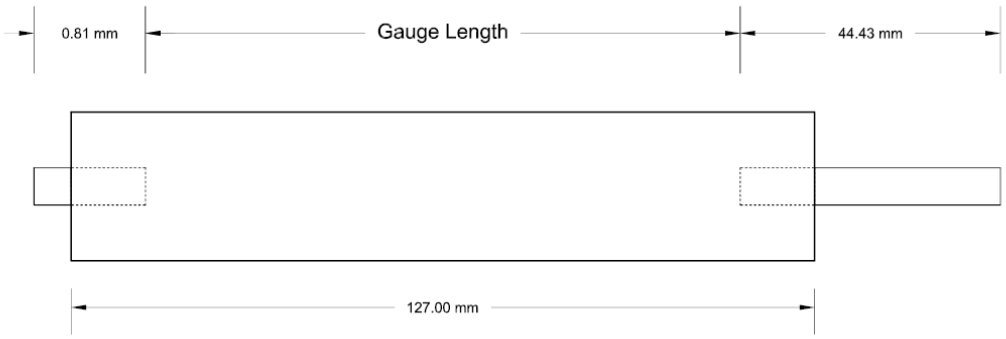

Figure 4.6 Prism assembly used for length measurement.

Table 4.3 Labeling system used for conditioned samples.

	Siloxane PD	Natural Stone Treatment	Control
45% RH	SL	NL	CL
75% RH	SH	NH	CH

Weight was measured using a Sartorius M-prove balance with a sensitivity of ±0.01 g. Measurement of length was taken using a HUMBOLT H3250 length comparator with a digital indicator (Figure 4.7). The sensitivity of the length comparator is ±0.002 mm. To measure the length, an adapter for 5" specimens was installed on the base. A reference bar was used to calibrate the length comparator to zero before each prism was measured. For each reading taken, the prisms were always placed in the same orientation in the length comparator to minimize changes in reading due to differences in contact surfaces. Reading with the same surface facing front as well as the minimum reading as the prism was rotated slowly in the comparator were both recorded.

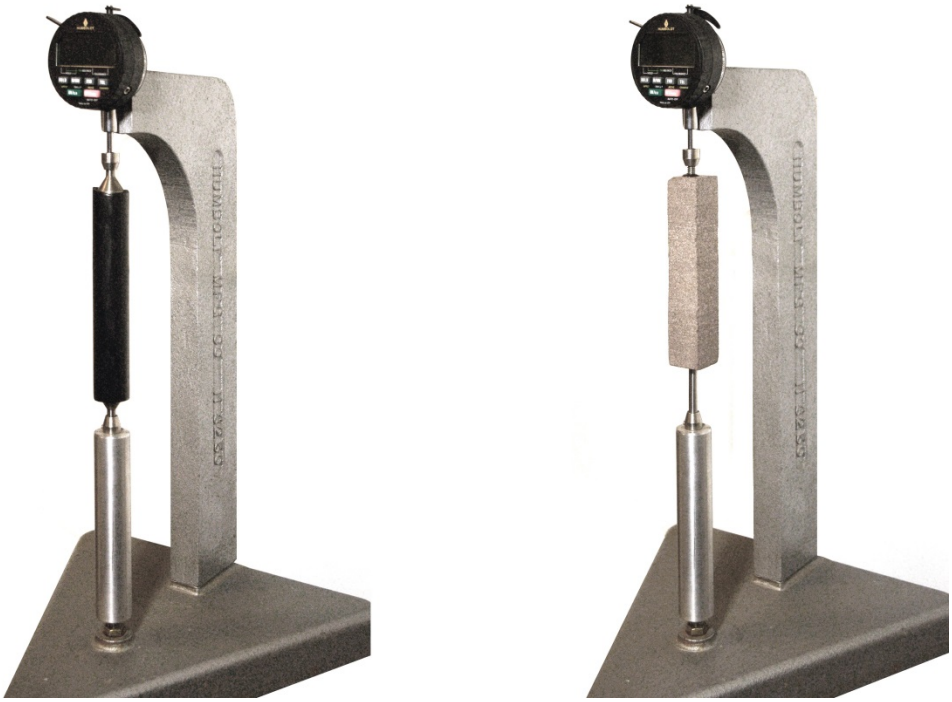

a b

Figure 4.7 Examples of HUMBOLDT length comparator with an adapter for 5" specimens installed on the base measuring (a) a reference bar in order to calibrate it to zero before each reading taken; (b) a prismatic specimen placed in the same orientation for each reading taken.

After the initial oven-dried weight values were obtained, the prisms were divided into two halves and put into the desiccators to condition them at 43 % RH and 75 % RH, respectively. Measurements of weight and length were both taken at three-day intervals until they were stabilized, which meant that differences between two successive measurements were less than 1 % of the average weight/length of the prisms. Once the prisms were equilibrated, the two water repellent agents were applied to all the surfaces immediately at the time the prisms were taken out of the

desiccators. One coat of each water repellent product was brushed on to saturation following the procedures described in the instructions provided by the manufacturer (Appendix E). The prisms were then allowed to dry on a hanger for about two weeks. Subsequently, their weight was recorded.

Then the prisms were dried in the oven again to obtain the dry weight values after the treatment. When they were equilibrated, all the prisms were subjected to moisture adsorption to obtain adsorption and expansion isotherms by being equilibrated in sequence at 43 % RH, 75 % RH, 98 % RH, as well as under total immersion in deionized water. Measurements of both weight and length were taken at three-day intervals and each stage was considered to be complete when the difference between two successive measurements was less than 1 % of the average weight/length of the prisms.

To process the data, absolute and relative amount of moisture adsorption and linear expansion at each RH level before and after the water repellent treatment was calculated. The results were plotted as isotherms using the average of three samples in each group with a standard deviation not greater than 10% of the mean. Comparisons were made between different RH levels as well as across the groups.

4.4 Water vapor transmission

The purpose of the water vapor transmission test is to determine the water vapor permeability of Portland brownstone, which expresses the steady water vapor movement in unit time through an area with parallel surfaces under specific temperature and humidity conditions. The test is used to evaluate any changes the water repellent treatment may have on the water vapor transfer of the sandstone.

Eighteen disks (⌀ 44.5 x 25.4 mm) were drilled out of a stone slab and were divided into groups of three, labeled with the same coding system as the prisms, shown in Table 4.3. After the initial oven-dried weight was obtained, the disks were conditioned at 43 % RH and 75 % RH respectively as labeled, until they were equilibrated gravimetrically. The conditioned disks were then treated with the two water repellent agents, Natural Stone Treatment and Siloxane PD (Table 4.2), on the top surface following the procedures described in the instruction provided by the manufacturer (Appendix E). After the treatment, the disks were allowed to dry on a rack for several weeks.

Twelve treated disks and three controls were selected for the subsequent testing using the Water Method based on ASTM E96. Sides of the selected disks were sealed with black electrical tape and attached as covers on 50 ml tri-cornered polypropylene cups with the treated surface facing up. The cups held 30 ml of deionized water and the assemblies were sealed using paraffin wax. A dummy

specimen attached to an empty cup in the normal manner was used to compensate for variability in test conditions. The assemblies were weighed and then set into the 43 % RH desiccator, so that a moisture flow occurred through the disks from the water to the controlled atmosphere. The loss in weight of the assemblies was measured every 24 hours to obtain 13 data points. The rate of Water Vapor Transmission (WVT) and Permeance were calculated from the obtained testing results.

4.5 Water absorption and drying behavior

The testing of water absorption and drying behavior consists of three parts: capillary water absorption, water absorption by total immersion, and drying. It aims to assess the liquid water absorption capacity of Portland brownstone, in order to characterize its open porosity. The procedure incorporates a variety of standards including NORMAL 11/85 and 29/88; ASTM C97-09 and C948-81; and the ICCROM ARC Laboratory Handbook 1999.

4.5.1 Capillary water absorption

Capillary water absorption was conducted using four untreated Portland brownstone blocks of approximately 50 x 50 x 50 mm in size. After obtaining the oven-dried weight of each block, they were placed on a sponge cloth saturated with

deionized water in a plastic container with a tight fitting lid. Each absorption surface orientation (parallel or perpendicular to the bedding) was represented by two blocks. As soon as the sample touched the water, track of the weight as a function of time was kept until the variation in the amount of absorbed water in two successive weighings at a 24-hour interval was equal or less than 1 % of the amount of total water absorbed.

The capillary water absorption curve was plotted and two parameters are calculated for capillary water absorption. The asymptotical capillary water absorption, expressed in g/cm^2, represents the total amount of water absorbed by capillarity per unit surface. The capillary absorption coefficient, which is the angular coefficient of the initial straight segment of the capillary absorption curve, is expressed in $g/cm^2\ s^{1/2}$. A correlation factor was calculated to define the confidence band.

4.5.2 Water absorption by total immersion and drying curves

For water absorption by total immersion and drying curves, the four blocks that had underdone the capillary absorption test were placed in a container and totally immersed in deionized water for 48 hours. Lightly patted dry on all sides, the blocks were weighed. Then the blocks were left to dry on a rack in a draft free environment. With the weight obtained by total immersion as a starting point, the

loss in weight was measured over a sequence of time as they dried. After the weight had reached an asymptotical value, the blocks were dried again in the oven, and this dry weight was used for the calculations of Total Water Content (U_0), Imbibition Capacity (IC), Water Absorption Capacity (WAC), and % Open Porosity.

The data for the drying curves was obtained by weighing each of the water saturated samples as they dried in the laboratory environment. The drying curves were plotted as moisture content versus time (day). The critical moisture content, the point where there is no longer capillary transport in the porous system, the initial drying rate as well as the final drying rate were calculated.

Chapter 5 Characterization of Portland brownstone and treatment application

5.1 Mineral composition

The composition and fabric of Portland brownstone were obtained by examination of thin sections of the stone under polarized light microscope. As shown in Figure 5.1 and 5.2, Portland brownstone consists essentially of quartz. The second most common minerals are a plagioclase feldspar (possibly albite) and mica, with iron oxides and clay being accessory minerals.

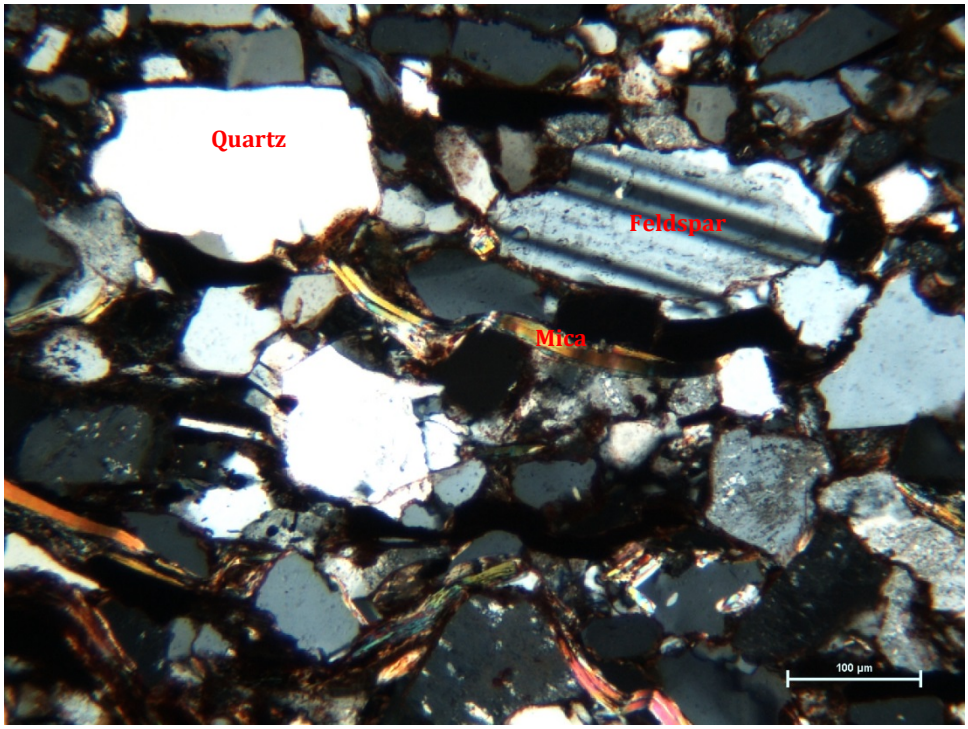

Figure 5.1 Photomicrograph showing the minerals present in the Portland brownstone.

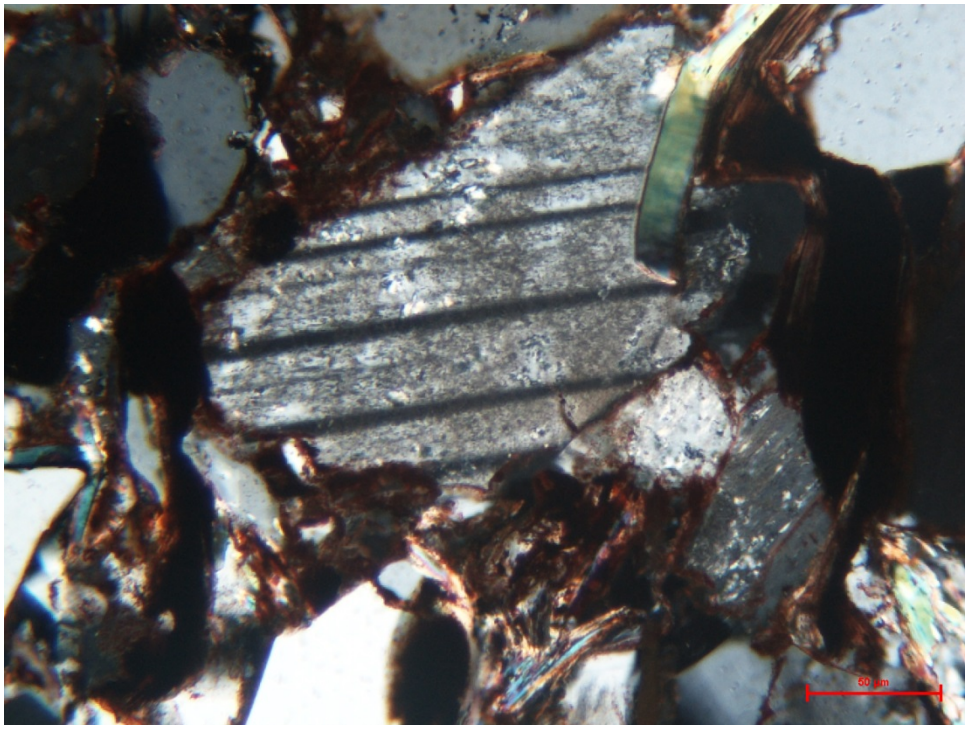

Figure 5.2 Photomicrograph of slightly altered plagioclase grain, showing albite twinning. Plagioclase will alter to mica and clay over time. The alteration is visible as a sort of fine grained grunge on the grain.

The presence of expansive clay minerals in the Portland brownstone was analyzed preliminarily through testing with methylene blue on a crushed and sieved sample (see section xx in previous chapter). Methylene Blue Absorption (MBA) and Cation Exchange Capacity (CEC) were calculated as follows.

MBA = [(X / Y) p] / (A / 100)

CEC = (np x 100) / A

Where,

X = weight of dried methylene blue crystals

Y = volume of diluted methylene blue solution

p = volume of methylene blue solution added

A = weight of sample

n = normality of methylene blue solution

Results of the experiment are given in Table 5.1. Most expansive clay minerals were detected among the particles finer than 0.075 mm in diameter. A rough calculation of MBA and CEC indicates a medium swelling potential of the particles finer than 0.075 mm, suggesting the adequate amount of expansive clays present among these particles that could be a deleterious feature for Portland brownstone. From what has been reported in literature (Jiménez González, Flatt, and Wangler 2012, 87; Wangler and Scherer 2008), these expansive clay minerals are likely to be vermiculite and smectite.

Table 5.1 Results of Methylene Blue Absorption and Cation Exchange Capacity on Portland brownstone.

Sieve No.	Particle Size (mm)	Sample (g)	Methylene Blue (ml)	MBA (g%)	CEC (meq./100g)
				MB Absorption	Cation Exchange Capacity
16	1.180	2.16	2	0.28	0.87
30	0.600	2.26	2	0.27	0.83
50	0.300	2.06	2	0.29	0.91
100	0.150	2.17	2	0.28	0.87
200	0.075	2.14	4	0.56	1.76
Pan	<0.075	2.13	8	1.13	3.53

Further information on the clay minerals was obtained through X-ray diffraction of the fines remaining in the pan after sieving. Comparison of the diffraction peaks detected (Figure 5.3) with a spectral database showed that kaolinite, chlorite, muscovite, and illite were the major clay minerals, which agrees with literature data provided by Wangler and Scherer (2009). The apparent disagreement in the larger amount of illite and muscovite in relation to chlorite could be attributed to the contribution made by the quartz peaks as this mineral had not been totally removed from the analyzed powder. None of the expansive clay minerals were identified. They would have required a more sophisticated sample preparation to detect them.

When the sample was glycolated with glycerol, no identifiable broadening and shifting of diffraction peaks was observed (Figure 5.4). However, all the major peaks identified as kaolinite, chlorite, muscovite, and illite were sharpened and increased in intensity. According to Moore and Reynolds (1997), kaolinite, chlorite, muscovite, and illite are unaffected by glycolation, while the peaks of vermiculite and smectite usually sharpen and increase in intensity (Moore and Reynolds 1997; Barshad 1950). Considering that vermiculite has spacings at 14.5Å, 7.2Å, 4.80Å and 3.58Å, similar to the characteristic lines of kaolinite (7.1Å and 3.57Å) and chlorite (14Å, 7Å, 4.72Å and 3.53Å), the increased intensities were likely to result from the

contribution of vermiculite, either present by itself or in the form of mixed layer clays.

Literature indicates that a small amount of smectite is also presents in Portland brownstone (Wangler and Scherer 2008). A slight shift to a higher d-spacing of the basal spacing on ethylene glycolation was expected but no obvious peak migration was observed. This might be due to the limited amount expansive clay minerals in this particular sample of Portland brownstone. It has been reported that Portland brownstone has clay content at approximately 3 %, with expansive clay content at only about 5 % of the clay content (Jiménez González, Flatt, and Wangler 2012, 37) at the edge of the detection level for XRD analysis. According to Weaver (1956), both tested and computed migration of the peaks of randomly interstratified mixed layer clays is very weak when the percentage of expanded layers is below 30% percent (Weaver 1956; Brown and MacEwan 1950). However, a close examination of the first-order peak identified as chlorite revealed that in the untreated specimen, it was actually moved toward a higher d-spacing value, likely to be the reflection resulting from the mixture of 14Å (chlorite) and 17Å (smectite) layers. In glycolated specimen, this peak had a subtle move toward 17Å, likely to be caused by the expansion of smectite on glycolation.

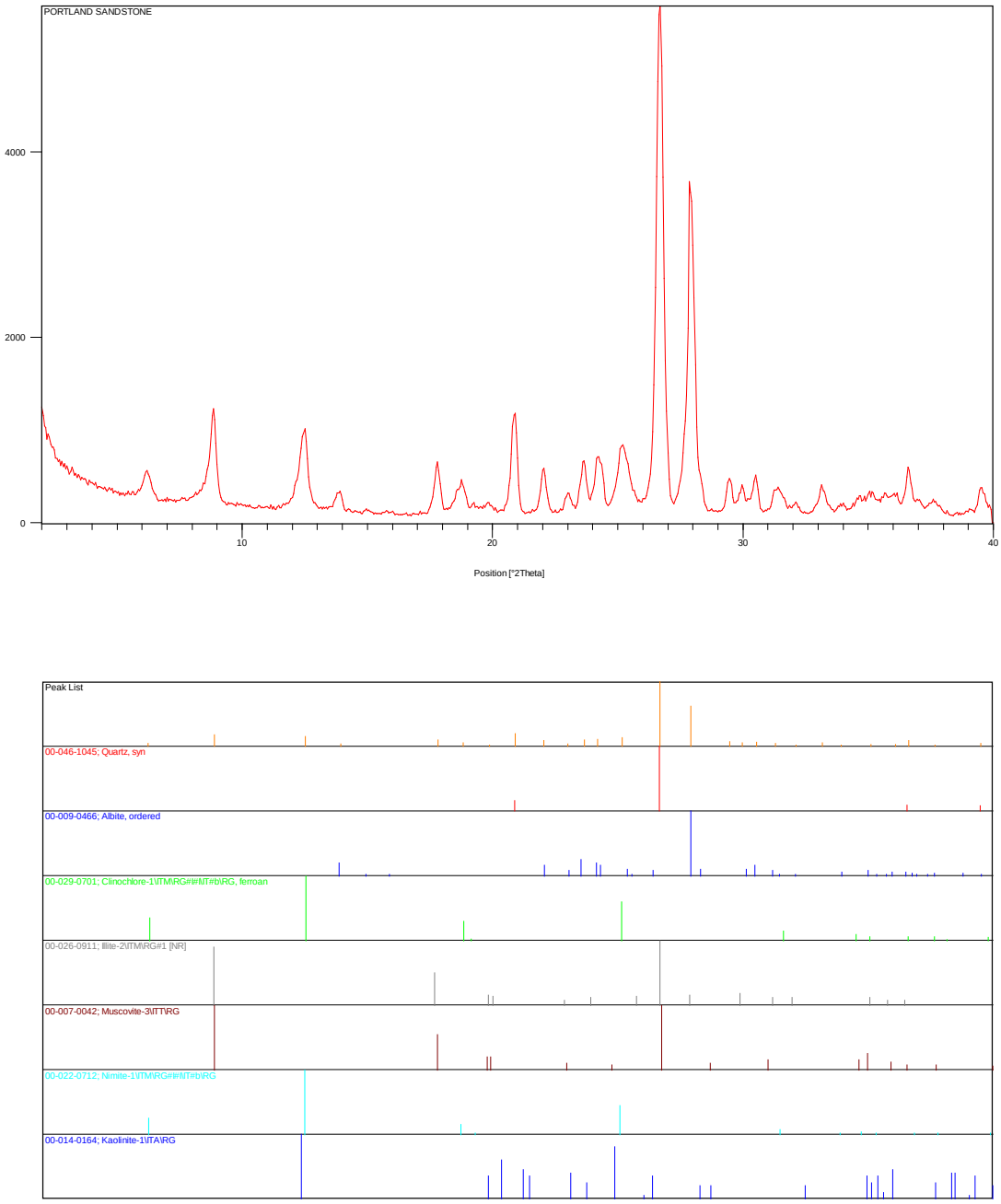

Figure 5.3 X-Ray powder diffraction pattern obtained from the fines of the ground Portland brownstone.

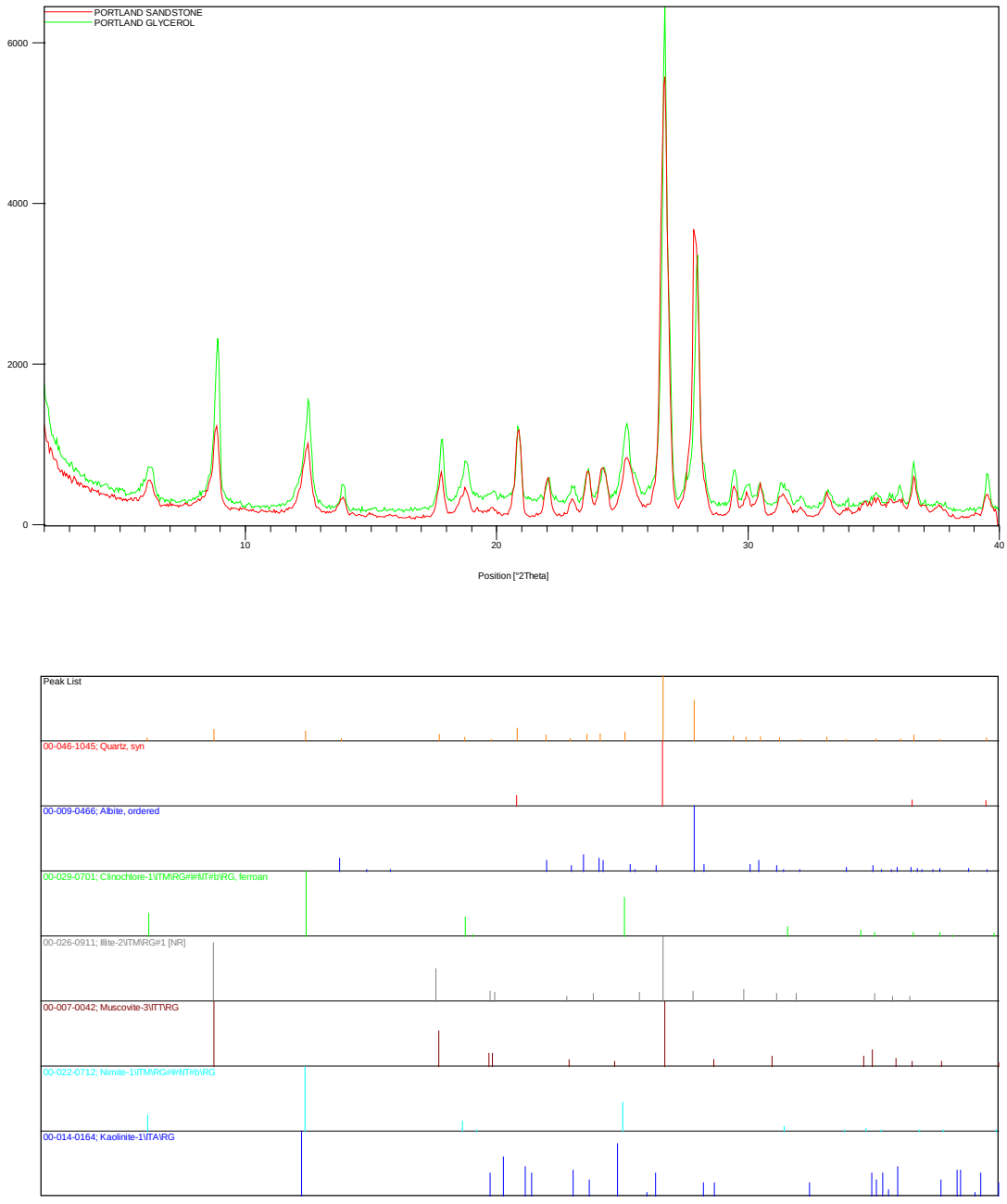

Figure 5.4 X-ray powder diffraction pattern for the sample treated with glycerol to show shifting of the expansive clay peaks. No significant changes were observed as the concentration of the expansive clays (around 5% of the clay content) is at the sensitivity limit of the instrument.

ESEM enabled a direct observation of this mixed layer chlorite-smectite (C/S) present in Portland brownstone. As shown in Figure 5.5, grains of quartz are covered by a thin coating of clays. The fine perpendicular honeycomb fabric is a typical look of mixed layer C/S (Worden and Morad, 2003). The elemental analysis by EDS targeted on this spot showed that the % Fe is similar to that of % Mg, while that of % Al is twice as much, which corresponds to the general formulas for C/S (Appendix F). Other than the grain-coating clays, micaceous clays, such as hydromuscovite (illite), are also evident in the interstices between grains. As shown in Figure 5.6, the mica and resulting micaceous clays are arranged tangentially to the grain surfaces, which might have effect on permeability since they usually sit within pores and pore throats (Worden and Morad 2003; Pallatt, Wilson, and McHardy 1984).

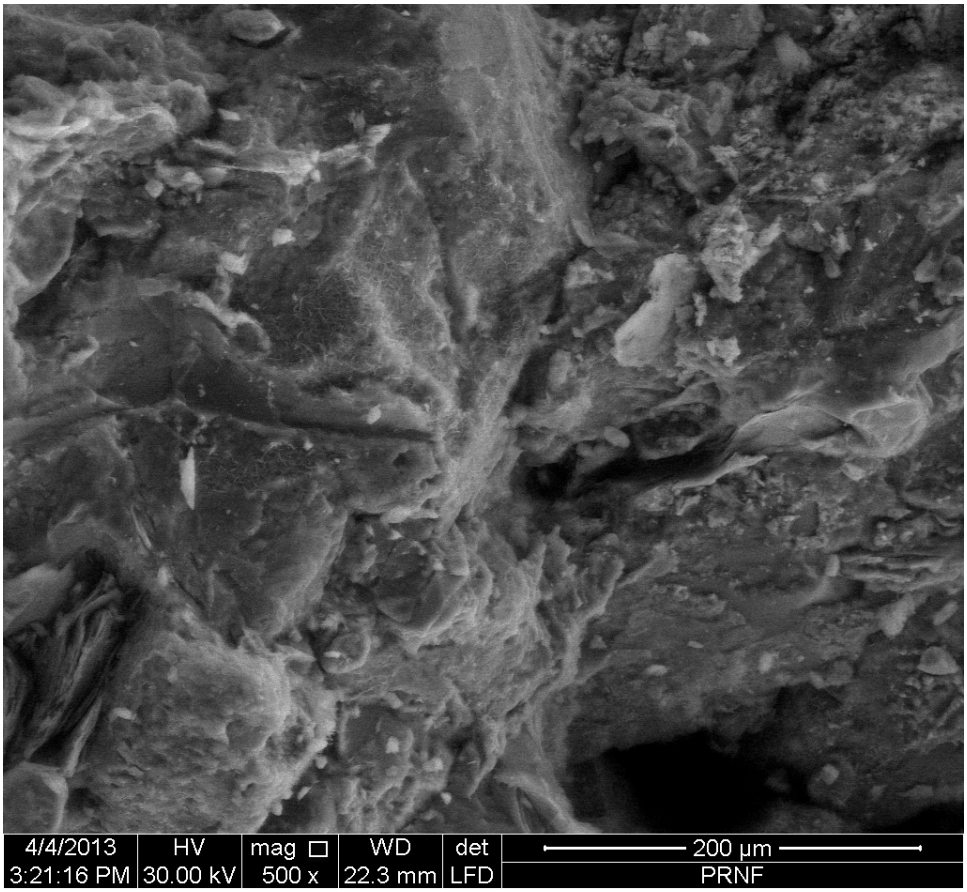

Figure 5.5 ESEM micrograph illustrating the mixed layer chlorite-smectite present as a fine perpendicular honeycomb fabric on the grain surfaces.

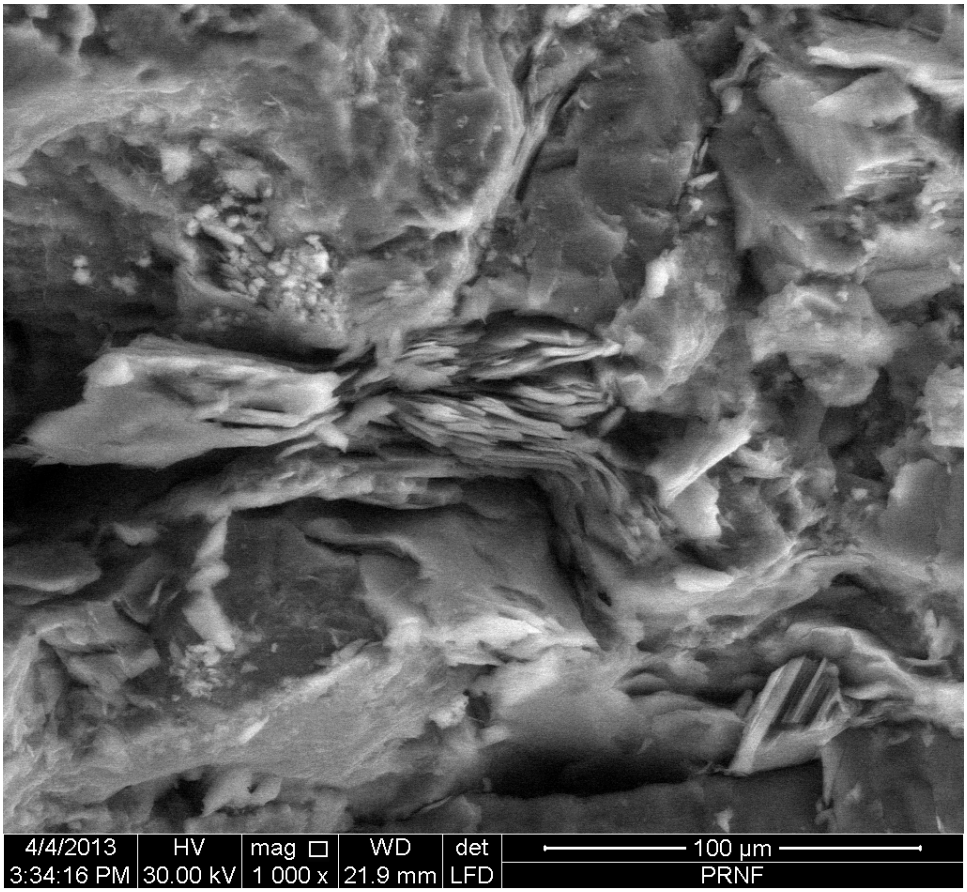

Figure 5.6 The mica, muscovite mixed with its weathering mineral, illite, are found in booklets between quartz grains.

5.2 Grain fabric

Figure 5.7 illustrates the particular microscopic structure of Portland brownstone. As shown in the picture, the sandstone is characterized by sub-angular to sub-rounded sedimentary particles, with some crystals grown in situ. The sizes of grains are nearly uniform throughout one bed, and greater variation is found in passing from one bed to another, which may be attributed to the sorting by water at the origin of the stone. Mica is oriented along the bedding plane, whereas quartz is

generally randomly oriented without preferred orientations being well developed. A relatively high compaction is evidenced by grain contacts located along grain boundaries. The interstitial spaces between the grains are mostly filled with matrix minerals and cement.

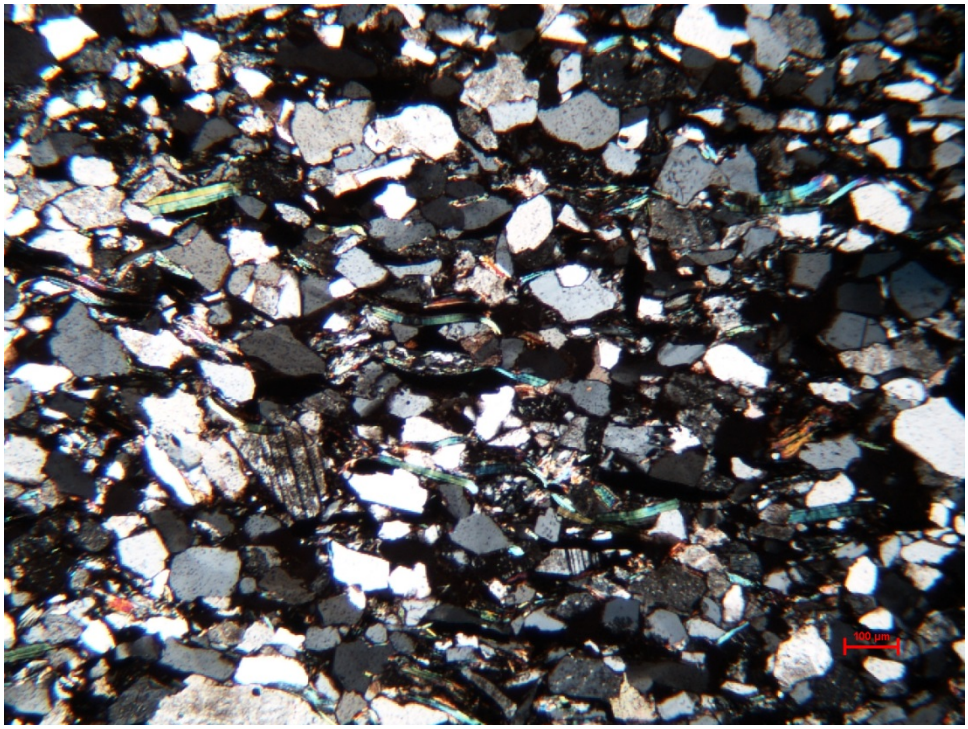

Figure 5.7 Microscopic structure of Portland brownstone showing the random orientation of quartz.

The grain size distribution was analyzed by dry sieving. The information obtained is summarized in Table 5.2 and plotted with a logarithmic graph in Figure 5.8. Although the grains of which Portland brownstone is composed varies in size, the grain size distribution is generally log-normal, there being as much aggregate

finer than the average as that coarser than the average. It is moderately sorted, with about 95% of the total particles included being sand. Most of the particles are of a medium size which ranges from 0.075 mm to 0.300 mm in diameter and that one-third of the grains are finer than 0.150 mm in diameter.

Table 5.2 Grain size information of Portland brownstone obtained by dry sieving.

Sieve No.	Particle Size (mm)	Sample Retained (g)	Percent Retained (%)	Percent Passing (%)
8	2.360	3.02	2.47	97.53
16	1.180	8.36	6.84	90.69
30	0.600	7.60	6.22	84.48
50	0.300	13.91	11.38	73.10
100	0.150	45.48	37.20	35.90
200	0.075	38.37	31.38	4.51
Pan	< 0.075	5.17	4.23	0.29

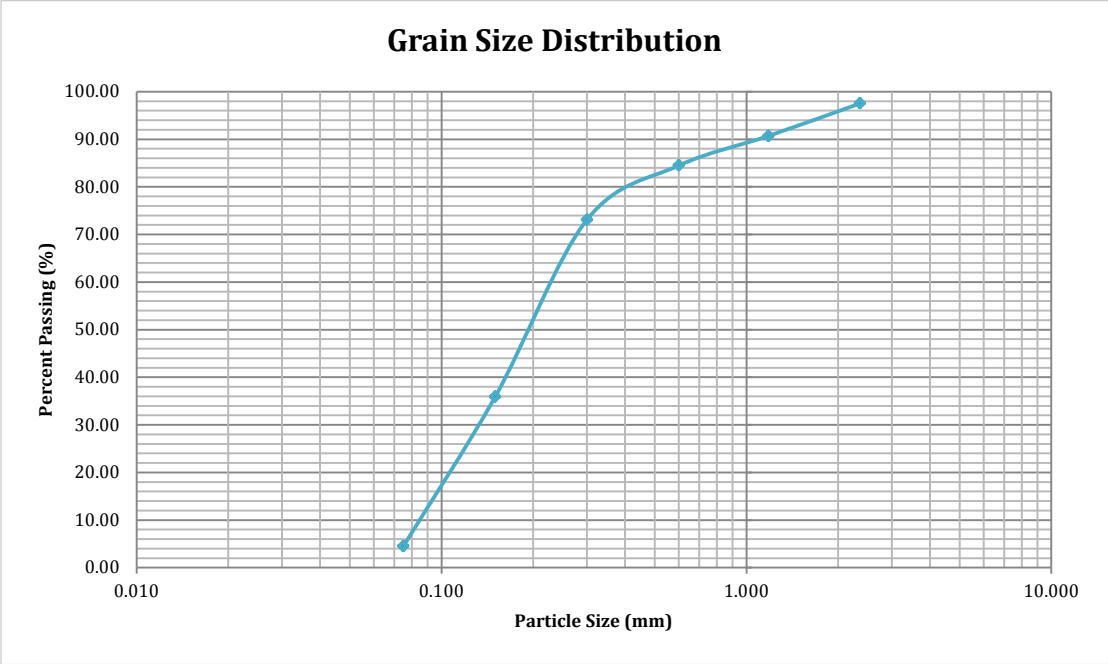

Figure 5.8 Grain size distribution graph for the crushed Portland brownstone.

5.3 Water absorption and drying

5.3.1 Capillary water absorption

The basic information of the four untreated blocks being tested for capillary water absorption is summarized in Table 5.3. Sample A and B were placed with the absorption surface parallel to the sedimentary bedding planes, whereas sample C and D were placed with the absorption surface perpendicular to the bedding planes. These samples also showed variations in weight, volume, and absorption surface area.

Table 5.3 Sample information for the capillary absorption test.

ABSORPTION SURFACE ORIENTATION	SAMPLE	INITIAL WEIGHT [$W_{i\text{-}dry}$ (g)]	DRY WEIGHT [W_{dry} (g)]	ABSORPTION SURFACE AREA [A_s (cm^2)]	VOLUME [V_s (cm^3)]
Parallel to bedding	A	346.23	345.37	27.19	142.04
	B	335.70	334.86	25.91	134.71
Perpendicular to bedding	C	352.06	351.20	28.44	148.96
	D	325.85	325.05	25.94	139.41

The capillary water absorption curve was plotted for each sample as shown in Figure 5.9. It shows a clear correlation between the capillary absorption surface orientation and the capillary absorption rate. Although not identical, two blocks laid in the same orientation generally showed the same trend in the curves; obvious differences were observed between different orientations in terms of capillary water absorption coefficient and the amount of time it took for them to equilibrate.

It took sample A and B about 136 hours to reach an asymptotical water absorption value, twice as much time as sample C and D did to reach that value.

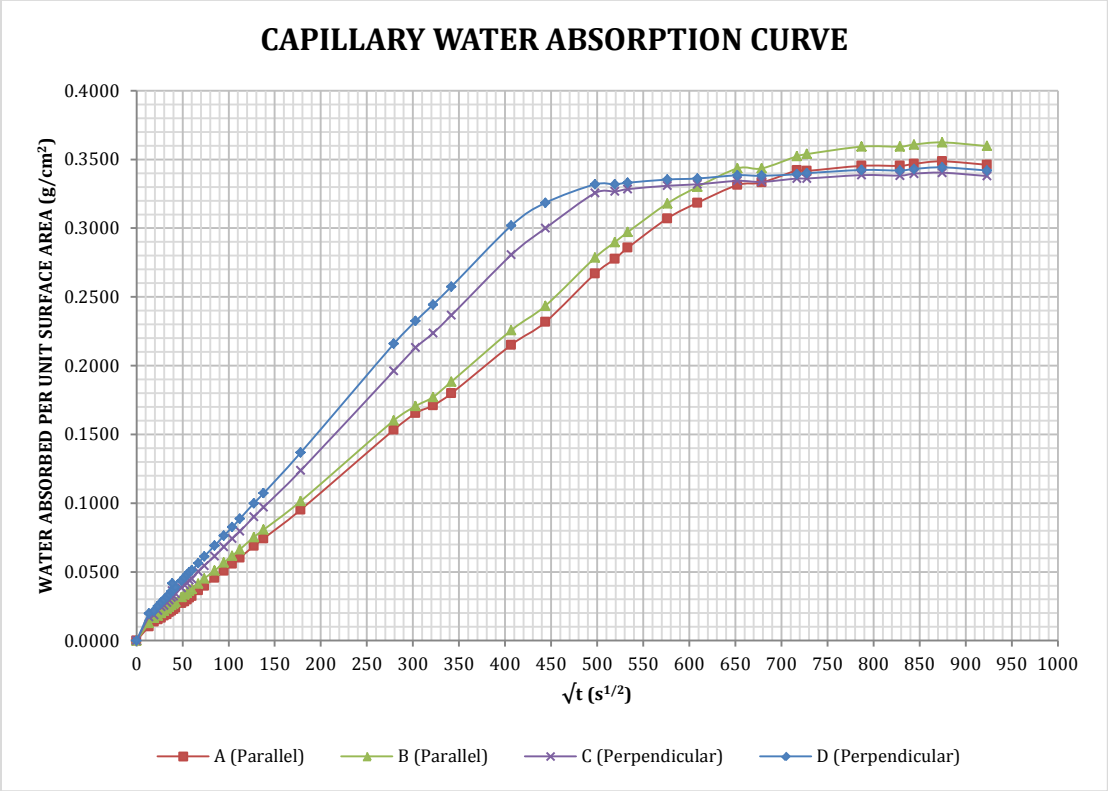

Figure 5.9 Capillary water absorption curve plots for all samples.

Table 5.4 shows the capillary absorption coefficient calculated as the slope of the straight section of the absorption curve, which reflects the initial capillary absorption rate. As shown in the table, the coefficient for sample C and D was higher than that of sample A and B, indicating a much faster water absorption rate along the sedimentary bedding planes. This corresponds to what is described in literature

that face bedded Portland brownstone shows a more rapid destruction (Bowles 1939, 73-74; Crosby and Loughlin 1904; United States Census Office 10th census 1883, 368). However, the asymptotical water absorption is similar for all the samples (Table 5.5), suggesting that there is no dependency of the total amount of capillary water absorption on the absorption orientation, which might lead to similar long-term results.

Table 5.4 Capillary water absorption coefficient for all samples.

ABS. SURFACE ORIENTATION	SAMPLE	CAPILLARY ABSORPTION COEFFICIENT		CORRELATION FACTOR
			AVERAGE	
Parallel to bedding	A	0.0005295	0.00054	0.9998
	B	0.0005446		0.9998
Perpendicular to bedding	C	0.0006785	0.00071	0.9997
	D	0.0007330		0.9996

Table 5.5 Asymptotical capillary water absorption for all samples.

ABS. SURFACE ORIENTATION	SAMPLE	ASYMPTOTICAL WATER ABSORPTION		
		U_{ta} (g)	M_a (g/cm^2)	AVER. M_a (g/cm^2)
Parallel to bedding	A	9.41	0.3461	0.35
	B	9.32	0.3597	
Perpendicular to bedding	C	9.61	0.3379	0.34
	D	8.87	0.3419	

5.3.2 Total immersion and drying

For water absorption by total immersion, it made no difference whether the stone was laid parallel or perpendicular to its bedding. For the experiment of water absorption by total immersion, Total Water Content (U_0), Imbibition Capacity (IC),

Water Absorption Capacity (WAC), and % Open Porosity were calculated as follows and the results are shown in Table 5.6.

$U_0 = W_{max} - W_{dry}$

$IC = (W_{max} - W_{dry}) / W_{dry}$

$WAC = (W_{max} - W_{dry}) \times 100 / W_{dry}$

$\%\ Open\ Porosity = V_{op} \times 100 / V_s$

Where:

W_{max} = mass of the block after 24-hour immersion

W_{dry} = mass of the oven-dried block after the testing of drying

V_{op} = volume of open pores estimated from the total water content

V_s = total volume of the block

Table 5.6 Results of Total Water Content, Imbibition Capacity, % Apparent Porosity, and % Open Porosity for all samples.

SAMPLE	24-HOUR IMMERSION W_{max} (g)	TOTAL WATER CONTENT [$U_0 = (W_{max} - W_{dry})$ (g)]	IMBIBITION CAPACITY (IC) [$W_{max} - W_{dry}] / W_{dry}$	%APPARENT POROSITY (%IC)	%OPEN POROSITY ($\%V_{op}/V_s$)
A	355.10	9.48	0.0274	2.74%	6.67%
B	344.57	9.48	0.0283	2.83%	7.04%
C	361.15	9.71	0.0276	2.76%	6.52%
D	334.30	9.03	0.0278	2.78%	6.48%
Average			0.0278	2.78%	6.68%

As a comparison to the asymptotical capillary water absorption, the extra water absorbed by total immersion was calculated absolutely and relatively to

sample volume and Total Water Content (Table 5.7). The extra water absorbed by total immersion by Portland brownstone is 0.0009 g/cm^3 and 1.33% of the total water content.

Table 5.7 Results of extra water absorbed by total immersion for all samples.

SAMPLE	$U_{0\text{-}r}$ (g)	U_{ta} (g)	EXTRA WATER ABSORBED BY TOTAL IMMERSION [$U_{ex} = (U_{0\text{-}r} - U_{ta})$ (g)]	EXTRA WATER ABSORBED/VOL [U_{ex}/V_s (g/cm^3)]	% RELATIVE EXTRA WATER ABSORBED [$U_{ex}/U_{0\text{-}r}$]
A	9.48	9.41	0.07	0.0005	0.74%
B	9.48	9.32	0.16	0.0012	1.69%
C	9.71	9.61	0.10	0.0007	1.10%
D	9.03	8.87	0.16	0.0011	1.77%
AVERAGE				0.0009	1.33%

Initial drying rate and final drying rate were calculated as the slopes of the straight parts of the curves. The critical moisture content (g/cm^3), the point at which there is no longer continuity in the capillary flow within the drying sample, is given by the last point of the initial drying rate curve. The moisture content ψ (g/cm^3) was also determined and the results are shown in Table 5.8. Portland brownstone has an initial drying rate of 0.0116 g/cm^{3}h and a final drying rate of 0.000040 g/cm^{3}h. The drying curves are shown in Figure 5.10.

Table 5.8 Results of the drying rate and critical moisture content for all samples. The correlation factors for the calculated slopes were 0.995 for the initial drying rates and 0.967 for the final drying rates.

SAMPLE	INITIAL DRYING RATE (g/cm^3h)	FINAL DRYING RATE (g/cm^3h)	CRITICAL MOISTURE CONTENT (g/cm^3)
A	0.0107	0.000042	0.591
B	0.0122	0.000041	0.636
C	0.0114	0.000042	0.597
D	0.0120	0.000036	0.585
AVERAGE	0.0116	0.000040	0.602

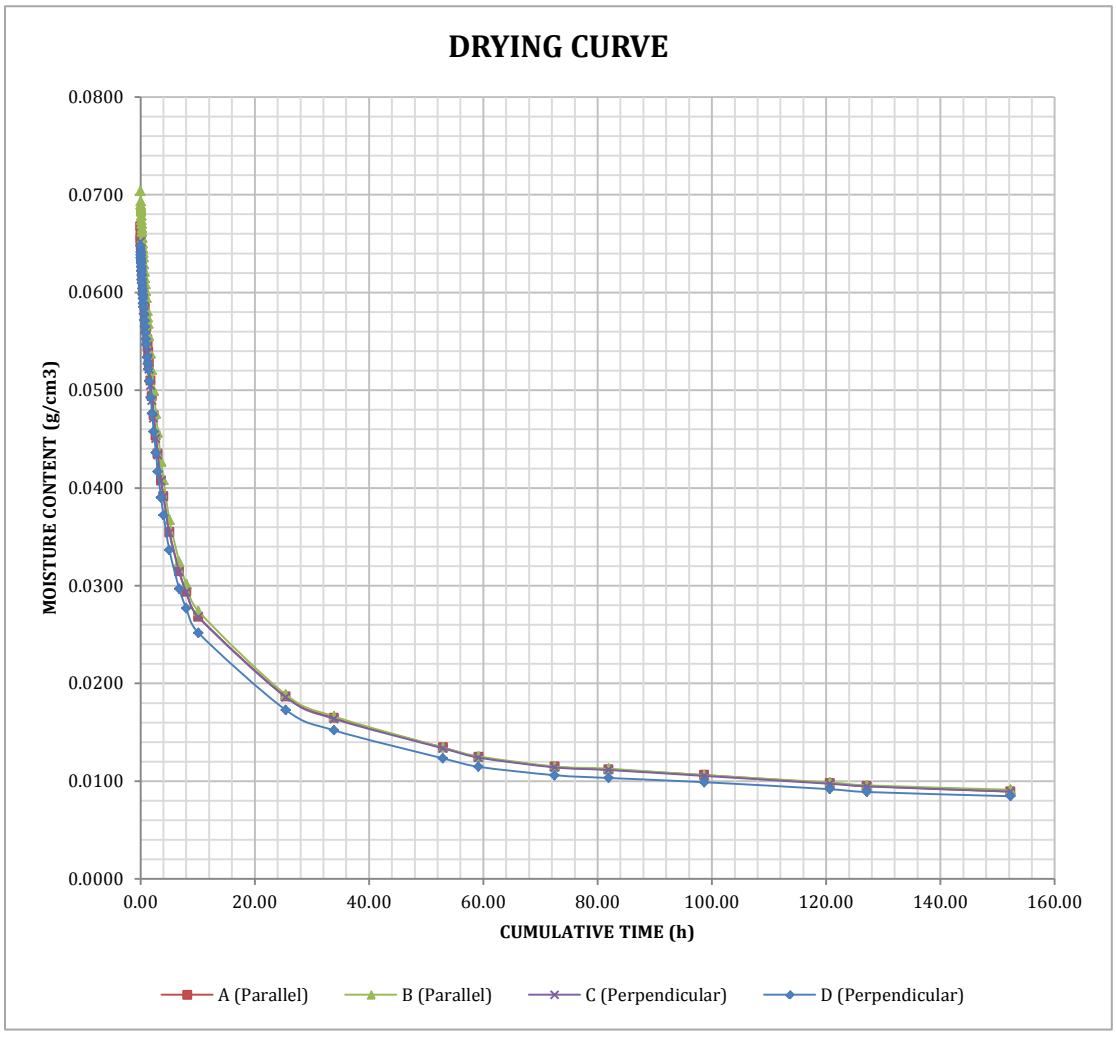

Figure 5.10 Drying curve plots for all samples.

5.4 Application of the water repellent

Both prismatic and disk shaped samples were treated with either one or the other water repellent once the specimens had been conditioned at either 43% or 75% RH. The water repellents, solvent based Natural Stone Treatment (NST) and water based Siloxane PD (SPD), were applied by brushing to saturation of the complete surface of the prisms and the top surface of the disks. One single coat was applied to each specimen. In the case of prisms, the amount of water repellent taken up by the samples was minimal and corresponded to relative weight increases between 0.02% and 0.03%.

ESEM images of the treated samples provide a detailed observation of the treatments with the two types of water repellent products. As illustrated in Figure 5.11 - 5.13, a smooth surface is achieved by either treatment.

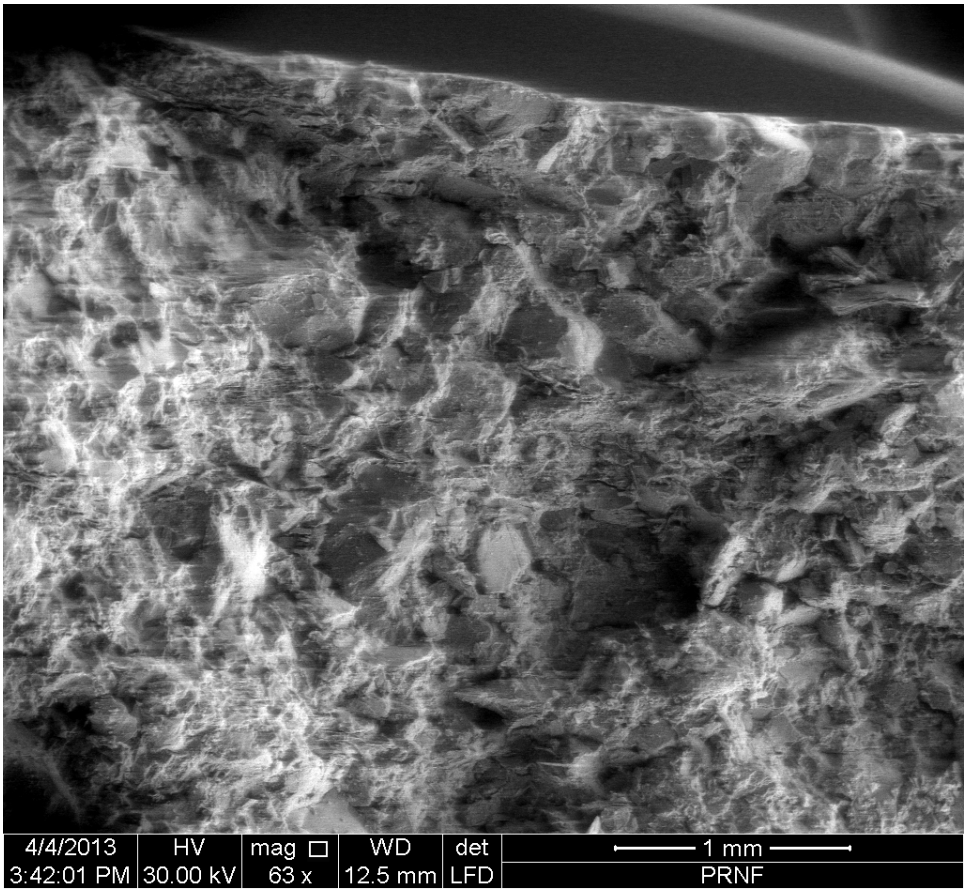

Figure 5.11 Portland brownstone brushed with one single coat of the solvent based NST water repellent seen as the thin layer on the surface of the cross-section.

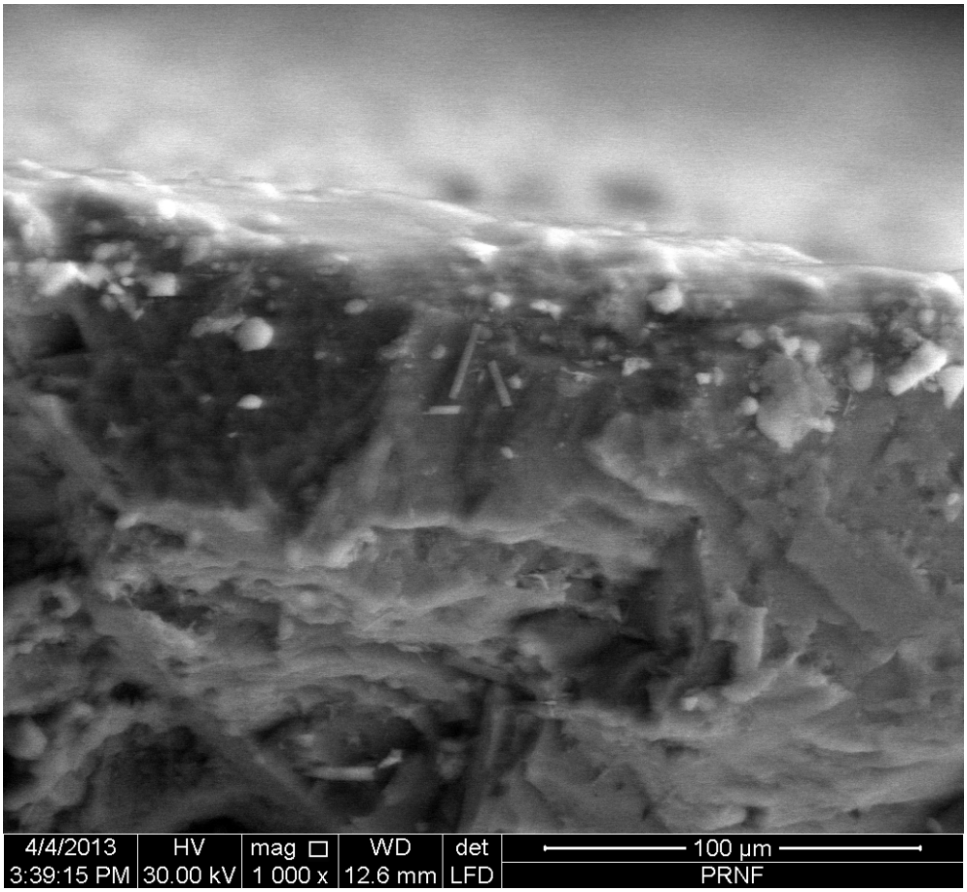

Figure 5.12 Detail of the above photomicrograph showing the micron thick surface coating of the solvent based NTS water repellent.

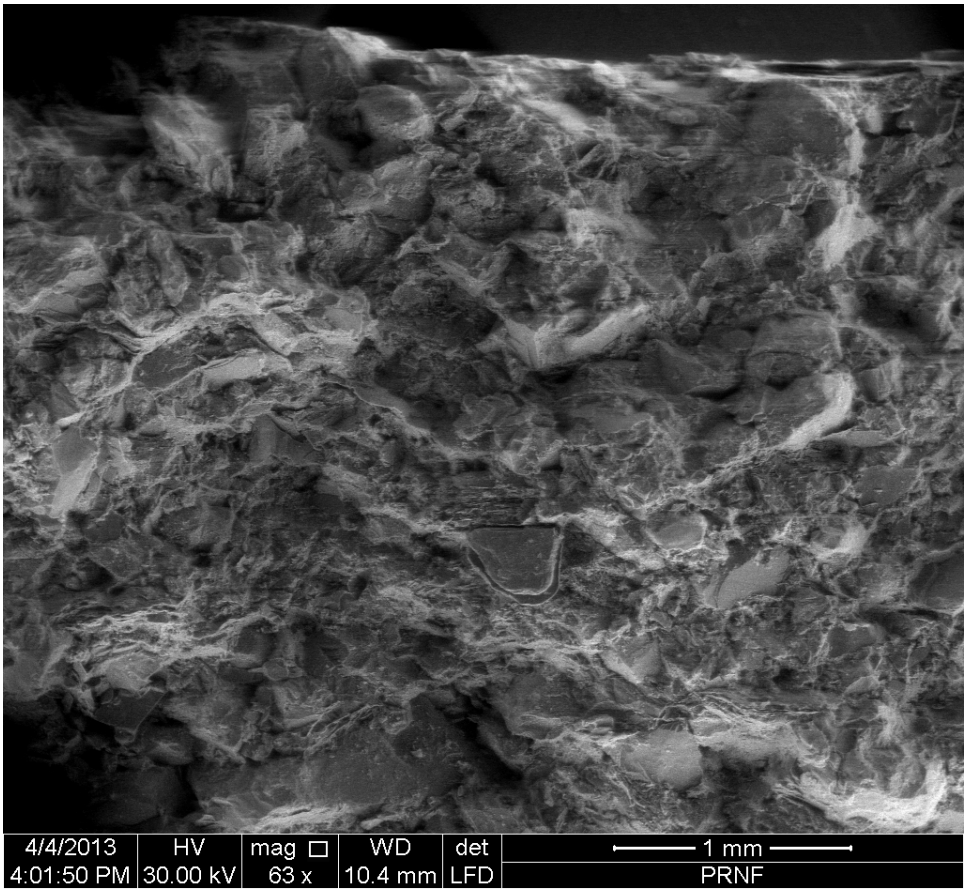

Figure 5.13 Portland brownstone tested with the water based SPD. The surface coating appears to be thinner.

To determine the depth of penetration of the water repellent, cross sections of the treated samples were wetted by spraying. As shown in Figure 5.14, the solvent based NST showed a better penetration depth (between 3 to 5mm) than the water based SPD (between 2 to 3mm) illustrated in Figure 5.15.

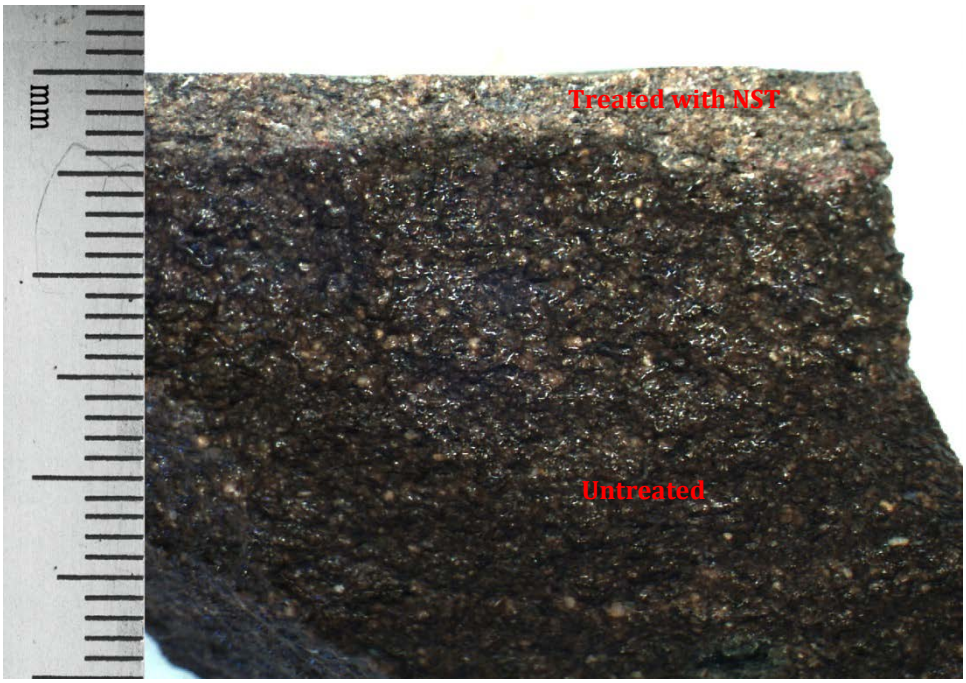

Figure 5.14 Portland brownstone tested with solvent based NST, showing an approximate penetration depth of about 5 mm for the product.

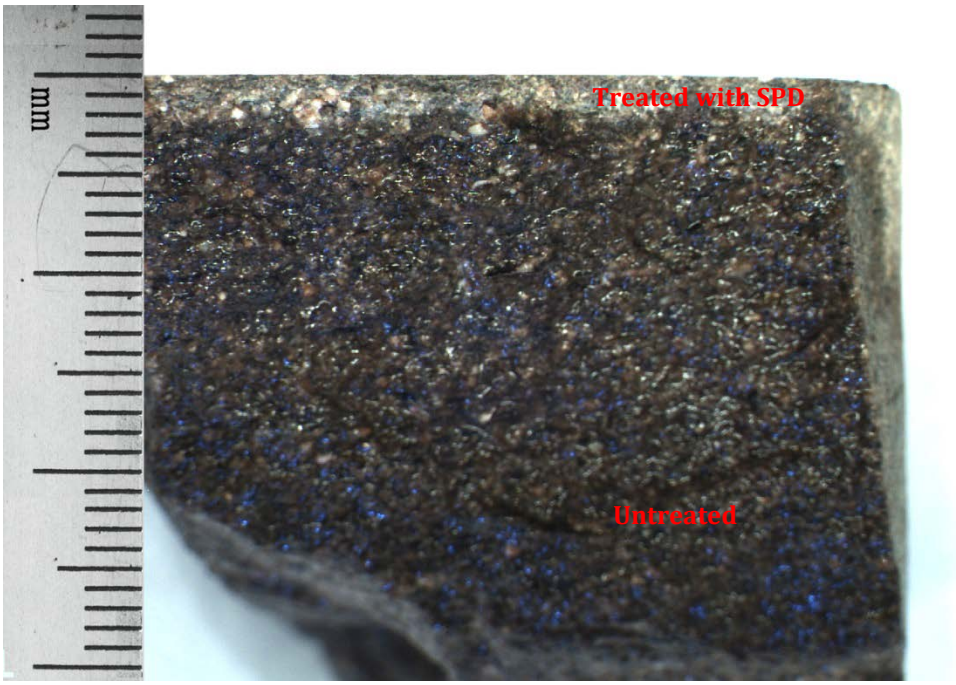

Figure 5.15 Portland brownstone tested with water based SPD, showing an approximate penetration depth of 2 mm of the product.

Chapter 6 Evaluation of the water repellent treatments

6.1 Introduction

Prismatic samples prepared from the Portland Sandstone were used to obtain the moisture adsorption curves and to evaluate the expansion of the sandstone. Six prisms were treated with the solvent based water repellent Natural Stone Treatment (NST) and another six with the water based water repellent Siloxane PD (SPD). Of these six, half were conditioned to 43% RH and the other half to 75%RH prior to the application of the water repellent. Six controls were used.

The water vapor permeability was determined on disk-shaped specimens, described in the previous chapter, where the top surfaces of six disks were treated following the same approach as for the prisms. Six were treated with one water repellent, half of them conditioned to 43% RH and the other half to 75%RH prior to the application of the water repellent. Three untreated controls were also tested.

6.2 Sorption isotherms

Results obtained from the moisture adsorption experiment are summarized in Table 6.1. Moisture adsorption was measured and calculated using the weight of the total assembly, stone prism plus pins, since the error introduced is constant. The values do not present the true adsorption amount of the stone but represent comparative results. The gained weight of the water repellent products was ignored through the calculations since it is less than 0.03% of the weight of the prism.

Table 6.1 Relative amount of moisture adsorption of treated and untreated samples, where SL= SPD @43%; SH= SPD @75%; NL= NST @43%, and NH= NST @ 75%.

	Control	SL	SH	NL	NH
0%	0.000	0.000	0.000	0.000	0.000
43%	0.124	0.121	0.115	0.119	0.124
75%	0.226	0.219	0.209	0.211	0.219
98%	0.607	0.519	0.552	0.596	0.510

The sorption isotherms are plotted as shown in Figure 6.1. The sorption pattern is comparable for all the samples, and the water repellent treatments did not appear to affect the amount of moisture adsorbed up to 75% RH. However, at 98% RH a significant increase in moisture absorption could be observed for all samples. The control, as usual, had the highest moisture adsorption, and the solvent based water repellent NST conditioned at 43 % RH, has practically the same absorption, while the equivalent sample conditioned at 75 % RH had the lowest adsorption. This value was similar to that of the water based SPD sample conditioned at 43 %, while that conditioned at 75 % adsorbed slightly more moisture, following the trend observed by Johansson (2008) in his study of concrete.

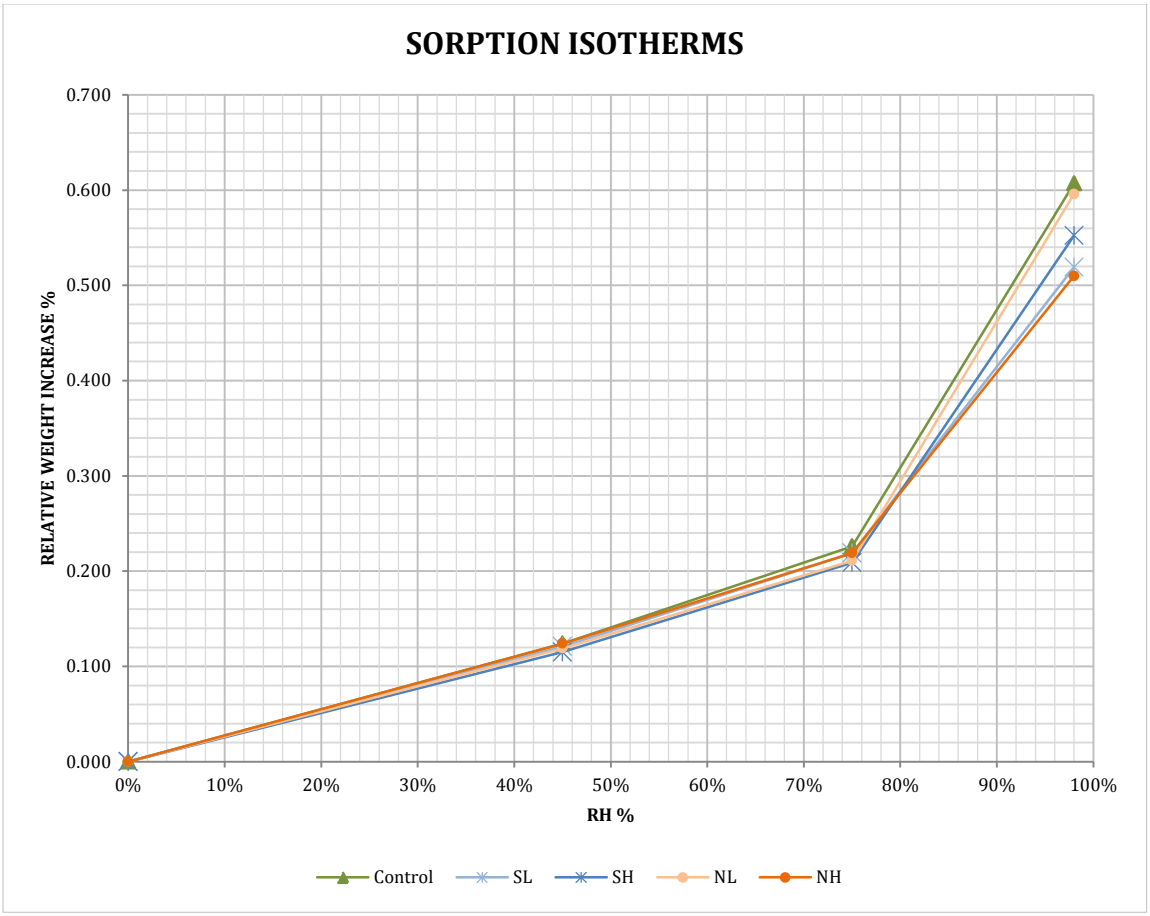

Figure 6.1 Sorption isotherms of treated and untreated prisms of Portland brownstone, where SL= SPD @43%; SH=SPD @75%; NL= NST @43%, and NH= NST @75%.

Between 0 % and 75 % RH, a fairly linear weight increase is evident on all the samples. Although subtle, negative deviation for the treated samples as compared to the untreated samples could be observed. The highest adsorption at 75 % RH was shown by the untreated samples with around 0.23 %. The samples treated with solvent based NST @ 43 % RH and those treated with water based SPD @75 % RH exhibited the lowest weight increase over this part of the humidity spectrum.

Because the conditioning chambers did not provide a uniform RH environment, particularly evident at the 98 % RH where condensation of water

vapor occurred on the surfaces of walls and shelves in the desiccator, the data show a rather wider spread. This effect was minimized by regularly changing the position of the samples, both on and between shelves, each time measurements were taken.

6.3 Linear expansion

The linear expansion was also measured at each RH and the results, expressed as relative linear expansion, i.e., change with respect to the original length, are presented in Table 6.2. Considering the sensitivity of length change to temperature fluctuation, data obtained when there was a temperature change of more than 5 °C were not considered.

Table 6.2 Relative linear expansion (mm/m) of treated and untreated samples, where SL= SPD @43%; SH= SPD @75%; NL= NST @43%, and NH= NST @ 75%.

	Control	SL	SH	NL	NH
0%	0.000	0.000	0.000	0.000	0.000
45%	0.024	0.024	0.020	0.032	0.028
75%	0.054	0.059	0.059	0.083	0.067
98%	0.127	0.123	0.131	0.163	0.143

The expansion isotherms are plotted in Figure 6.2. Unlike what was observed for the moisture adsorption, the expansion measured for all samples varied with the changes of RH and this can be attributed to the high sensitivity of the measuring system. Both solvent based NST treated samples expanded more than the water based SPD ones. The NST @ 43 % expanded more, following the higher amount of moisture adsorbed. However, the NST @ 75% which had adsorbed less water,

expanded more. This suggests that this solvent based water repellent induces extra swelling as has been noticed for other products (Bachem and Littmann 2001). On the other hand, the water based SPD expands more when conditioned at 75% RH than when conditioned at 43% RH, following the amount of moisture adsorbed.

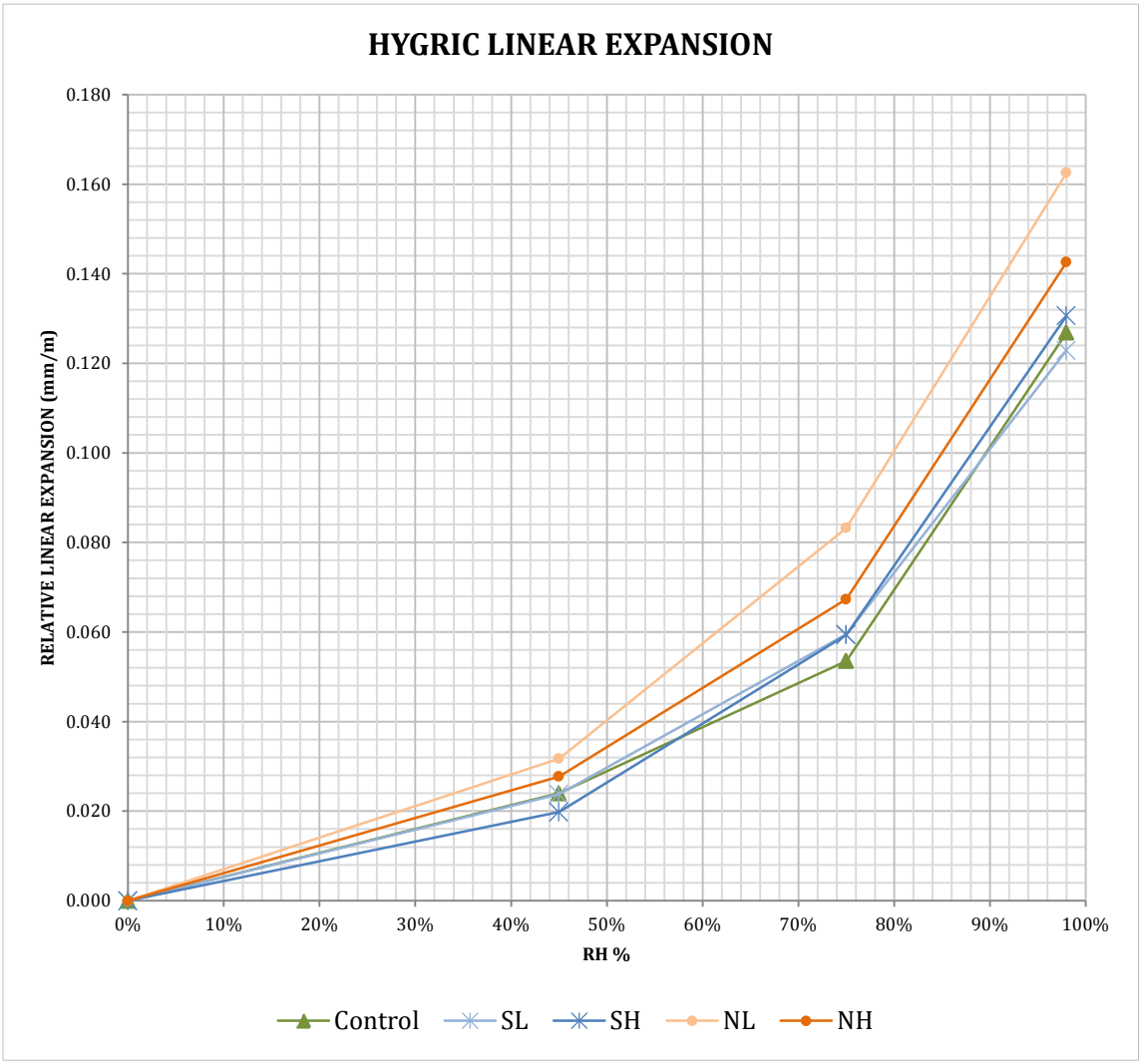

Figure 6.2 Expansion isotherms of treated and untreated prisms of Portland brownstone, where SL= SPD @43%; SH=SPD @75%; NL= NST @43%, and NH= NST @75%.

6.4 Water vapor transmission

In the water vapor transmission experiment, all of the samples exhibited a slight initial fluctuation in weight during the first three days, so that the last ten data points were used for graphic and numerical analyses. Considering the stability of the environmental condition reflected in the dummy specimen, data obtained were adjusted by reversing the direction of the dummy's weight change relative to its initial value.

The results of the experiment are summarized in Table 5.5, and average transmission curves are plotted in Figure 5.6, and the linear average slopes in Figure 5.7. The calibrated change in weight was plotted as function of elapsed time and the slope of the straight line was calculated to represent the rate of water vapor transmission (WVT). A correlation factor no less than 0.995 was required to define the confidence band. Permeance was calculated as follows:

Permeance = WVT / S ($R_1 - R_2$)

Where:

S = saturation vapor pressure at test temperature, mm Hg (1.333×10^2 Pa)

R_1 = relative humidity at the source expressed as a fraction

R_2 = relative humidity at the vapor sink expressed as a fraction

Table 6.3 Results of the experiment of Water Vapor Transmission showing calculations for WVT and Permeance, where SL= SPD @43%; SH=SPD @75%; NL= NST @43%, and NH= NST @75%.

Thickness (m)		0.0254			
Test area (m^2)		0.0015			
		WVT (g/m^2h)	Ave. WVT (g/m^2h)	Permeance (g/m^2hPa)	Ave. Permeance (g/m^2hPa)
SL	SL1	1.3698	1.17	1.81E-04	1.55E-04
	SL2	0.9660		1.28E-04	
	SL3	1.1750		1.55E-04	
NL	NL1	1.1560	1.12	1.53E-04	1.48E-04
	NL2	1.0762		1.42E-04	
	NL3	1.1308		1.49E-04	
SH	SH1	1.1780	1.08	1.56E-04	1.42E-04
	SH2	1.0486		1.38E-04	
	SH3	1.0038		1.33E-04	
NH	NH1	1.1588	1.28	1.53E-04	1.69E-04
	NH2	1.4954		1.98E-04	
	NH3	1.1866		1.57E-04	
Control	C1	1.3301	1.25	1.76E-04	1.66E-04
	C2	1.3185		1.74E-04	
	C3	1.1151		1.47E-04	
Average			1.18		1.56E-04

The results show that all the samples being tested exhibited similar water vapor transmission properties, varying within 10% of the average WVT of 1.18 g/m^2h and the average Permeance of 1.56E-04 g/m^2hPa. This agrees with literature that siloxane based water repellent agents do not “seal” the surface but allow water vapor to pass through.

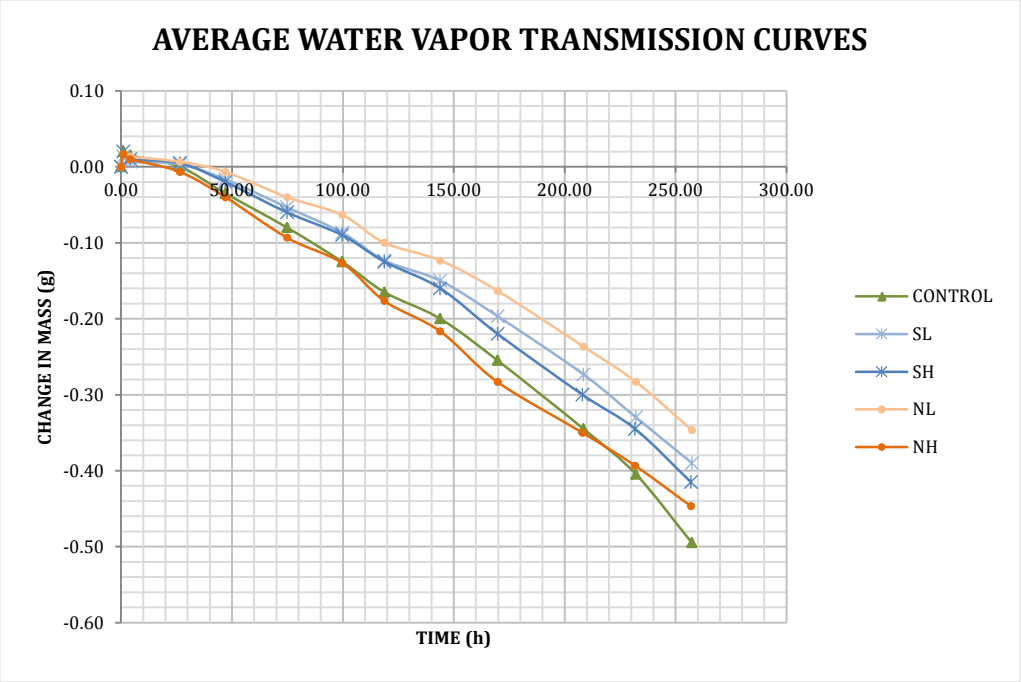

Figure 6.3 Average water vapor transmission curves, where SL= SPD @43%; SH=SPD @75%; NL= NST @43%, and NH= NST @75%.

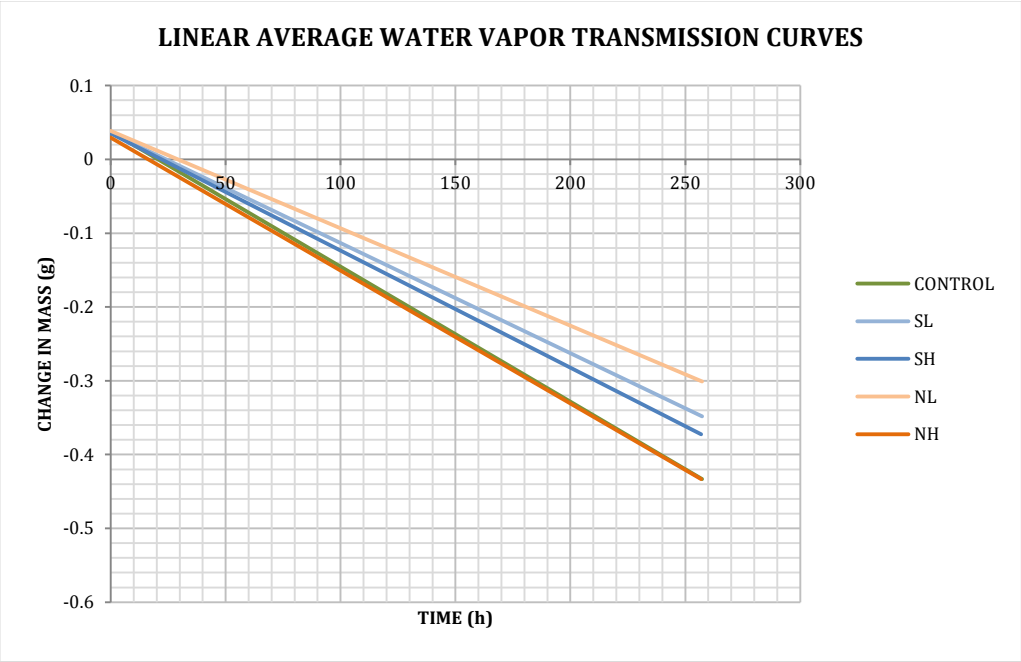

Figure 6.4 Linear trend lines of average water vapor transmission, where SL= SPD @43%; SH=SPD @75%; NL= NST @43%, and NH= NST @75%.

It was found that variations occurred between the two water repellent types as well as the moisture content at the time of application. For example, the solvent based NST applied to samples conditioned to 75% RH shows practically the same performance as the untreated control sample. On the other hand, the same product, applied to samples conditioned at 43% RH, showed the lowest water vapor permeability. The water based SPD treated samples fall in between these two, and again, the one conditioned at 75% RH shows the highest water vapor permeability.

In general, samples treated with either water repellent agent had lower water vapor transmission and permeance than the untreated samples, suggesting that in practice siloxane based water repellent agents may decrease somewhat the water vapor permeability of Portland brownstone. The higher water vapor permeability and permeance of the samples that were treated when conditioned to a higher moisture content suggests that the adsorbed moisture on the pore walls partially hinders the attachment of the water repellent agent so that “open paths” remain in the treated sample.

Chapter 7 Data Analysis and Conclusions

7.1 Summary of results

The results obtained can be summarized as follows:

—Water vapor adsorption: All samples followed the typical adsorption pattern where the amount of moisture adsorbed increased significantly for relative humidity above 75 %. At 98 % RH, the solvent based NST water repellent applied at 43 % showed an adsorption similar to that of the control, while the corresponding sample for the 75 % conditioning, showed the lowest adsorption. On the other hand, the water based SPD water repellent showed the expected pattern, with the one conditioned at 75 % RH adsorbing more than that conditioned at 43 % RH, which had the same low value as NST conditioned at 75 % RH.

—Hygric Linear Expansion: The solvent based NST water repellent applied at 43 % RH showed the highest expansion, as for the case of the adsorption pattern, followed by that applied at 75 % RH. However, the control, which had adsorbed the highest amount of moisture, showed a lower expansion, falling in between that measured for the water based SPD conditioned at 75 % RH and that conditioned at 43 % RH, which had the lowest value of all.

—Water vapor transmission: The control and the sample treated with the solvent based NST at 75 % RH showed the highest water transmission rate, followed by the water based SPD treated at 75 % RH, then by that at 43 % RH. The lowest rate was that of the solvent based NST applied on samples conditioned at 43 % RH.

7.2 Data Analysis

To determine whether the observed differences between the data were significant or not, statistical analyses were applied. The ***t*** Student test between pairs of data was used to compare the water vapor transmission rate. A complete cross analysis of all the sets was carried out, as reported in Table 7.1, and showed that there is a significant difference between the samples treated by the solvent based NST water repellent applied at a 43% RH moisture content and the water based SPD applied at 75% RH at the 95% confidence level (at 4 degrees of freedom). The next highest value, though not statistically significant is that for the same NST sample and the control, as expected when comparing the results obtained (Table 6.3 and Figure 6.3 in chapter 6).

Table 7.1 Results of the t-test for the water vapor transmission data. The t-value from the table corresponding to 2 degrees of freedom is equal to 2.78 at a 95% confidence level (4 degrees of freedom).

	SL	SH	NL	NH	C
SL					
SH	0.73				
NL	0.79	***3.10***			
NH	0.59	1.48	1.44		
C	0.69	2.04	2.16	1.38	

When an overall analysis of variance, ANOVA, was carried out for all the combined data as reported in Table 7.2, it could be confirmed that there is no significant difference between the water vapor transmission rates of the various samples at a 95% confidence level.

Table 7.2 ANOVA results from the comparison of all the WVT data at 98%RH. The F value from statistical tables is provided at a 95% confidence level (or 0.05 probability level).

	Sum of Squares	Degrees of Freedom	Mean Squares
Between treatments	0.089514	1	0.022378
Within treatments	0.200308	7	0.028615
		F_{exp}	0.782
	95% CL	F_{table}	5.59

A similar approach was used to analyze the data for both moisture adsorption and hygric linear expansion. In both cases, the data were compared pair-wise, and for the complete data set. Table 7.3 presents the obtained results of the pair wise comparison of the moisture adsorption at 75 % RH using analysis of variance.

Table 7.3 Pair-wise comparison of the moisture adsorption at 75 % RH data using ANOVA. At a 95% confidence level, the F value from the table is 7.72 for 1 and 4 degrees of freedom, numerator and denominator respectively. For the comparison with the control samples, the F value is 5.59 for 1 and 7 degrees of freedom.

	SL	SH	NL	NH	C
SL					
SH	5.14				
NL	3.20	0.14			
NH	0.00	6.64	3.96		
C	***7.57***	***48.38***	***35.84***	***9.40***	

The results clearly show that the control samples are absorbing a significantly higher amount of moisture than any of the treated ones, even though from the data (see Table 6.1 and Figure 6.1 in Chapter 6) this is not readily evident. The result of the analysis of variance comparing all treatments is presented in Table 7.4 and confirms that indeed there is a significant difference between the data.

Table 7.4 ANOVA results from the comparison of all the weight increase data at 75 %RH. The F value from statistical tables is provided at a 95% confidence level (or 0.05 probability level).

	Sum of Squares	Degrees of Freedom	Mean Squares
Between treatments	0.0008030	4	0.0073471
Within treatments	0.0002910	13	0.1156988
		F_{exp}	***8.97***
	95% CL	F_{table}	3.18

The process was repeated for the data at 98 % RH. Table 7.5 gives the pairwise comparison of the data. It can be seen, there is a significant difference between the moisture adsorption values for the solvent based NST water repellent depending on whether the product was applied at 75 % RH or at 43 % RH, the latter absorbing more moisture. The control sample had a slightly higher moisture adsorption than this last sample, however, there appears to be no significant difference between it and the lowest value corresponding to the NST at 75 % RH. This could be explained by the higher number of control samples, so that statistically this difference is not significant at that confidence level, although it has the highest value.

Table 7.5 Pair-wise comparison of the moisture adsorption at 98 % RH data using ANOVA. At a 95% confidence level, the F value from the table is 7.72 for 1 and 4 degrees of freedom, numerator and denominator respectively. For the comparison with the control samples, the F value is 5.59 for 1 and 7 degrees of freedom.

	SL	SH	NL	NH	C
SL					
SH	0.66				
NL	5.10	1.06			
NH	0.12	1.32	***8.73***		
C	3.77	1.34	0.06	4.82	

The analysis of variance taking into account all moisture sorption data for samples conditioned at 98 % RH is reported in Table 7.6 and shows that overall there is no significant difference in the moisture absorption at 95 % confidence level and the degrees of freedom involved.

Table 7.6 ANOVA results from the comparison of all the weight increase data at 98%RH. The F value from statistical tables is provided at a 95% confidence level (or 0.05 probability level).

	Sum of Squares	Degrees of Freedom	Mean Squares
Between treatments	0.0293883	4	0.0073471
Within treatments	1.5040846	13	0.1156988
		F_{exp}	1.74
	95% CL	F_{table}	3.18

For the case of the hygric linear expansion, a similar approach was used and an analysis of variance was applied to the data pairs. In Table 7.7 the results for the pairwise comparison of data at 75 % RH are presented. It is clearly evident that there are significant differences in the length increase for the solvent based NST treatment applied at the two different moisture contents, as well as between the samples treated at 43 % relative humidity and the control, and either of the water based SPD samples.

Table 7.7 ANOVA results from the pair-wise comparison of the linear expansion at 75% RH. At a 95% confidence level, the F value from the table is 7.72 for 1 and 4 degrees of freedom, numerator and denominator respectively. For the comparison with the control samples, the F value is 5.59 for 1 and 7 degrees of freedom.

	SL	SH	NL	NH	C
SL					
SH	0.00				
NL	***11.86***	***12.27***			
NH	0.98	0.98	***17.09***		
C	0.05	0.05	***11.08***	1.51	

However, when comparing all the data for 75% conditioning, shown in Table 7.8, no significant differences can be observed at the 95% confidence level.

Table 7.8 ANOVA results from the comparison of all the linear expansion data at 75%RH. The F value from statistical tables is provided at a 95% confidence level (or 0.05 probablility level).

	Sum of Squares	Degrees of Freedom	Mean Squares
Between treatments	0.0019012	4	0.0004753
Within treatments	0.0022925	13	0.0001763
		F_{exp}	2.70
	95% CL	F_{table}	3.18

At 98 % RH the hygric linear expansion data, presented in Table 7.9, shows again a significant difference between the water based SPD and the solvent based NST with samples conditioned at 43 % RH. The NST conditioned at 43% also shows a significant difference in expansion with the control samples.

Table 7.9 ANOVA results from the pair-wise comparison of the linear expansion at 98% RH. At a 95% confidence level, the F value from the table is 7.72 for 1 and 4 degrees of freedom, numerator and denominator respectively. For the comparison with the control samples, the F value is 5.59 for 1 and 7 degrees of freedom.

	SL	SH	NL	NH	C
SL					
SH	0.55				
NL	***9.21***	6.54			
NH	6.25	3.03	3.67		
C	0.10	0.09	***7.19***	1.69	

However, the ANOVA applied to take into account all the samples, does not show a significant difference as can be seen in Table 7.10.

Table 7.10 ANOVA results from the comparison of all the linear expansion data at 98%RH. The F value from statistical tables is provided at a 95% confidence level (or 0.05 probability level).

	Sum of Squares	Degrees of Freedom	Mean Squares
Between treatments	0.0033371	4	0.0008343
Within treatments	0.0635569	13	0.0048890
		F_{exp}	2.48
	95% CL	F_{table}	3.18

7.3 Conclusions

The study has shown that when considering the overall data no significant differences were observed between the two types of water repellent treated samples and the controls, for water vapor permeability, as well as for moisture adsorption and linear elongation measured at 98% RH. However, for samples conditioned at 75% RH, while there was a significant difference in moisture adsorption, none was found for the hygric linear elongation.

However, significant differences were found for all the parameters measured between the solvent based NST and the water based water SPD when these were applied on sandstone samples conditioned at 43% RH, except for moisture sorption at 75% RH, where all of treated samples differed from the controls, which may reflect that the former may not have reached equilibrium (the data were obtained in the summer and temperature fluctuated highly in the laboratory).

Considering the linear hygric expansion, the water based SPD showed the lowest values, with that treated at 75% RH absorbing more moisture than when treated at 43% RH, following the study by Johansson (2008). On the other hand, the solvent based NST water repellent showed the highest expansion, even more than

the control, although it had adsorbed as much moisture, so that this effect is a result of the presence of this product.

The two formulations tested differ in whether the siloxane is in solution with the solvent or in an aqueous dispersion. From the results obtained, the solvent based product applied at samples conditioned at a higher RH showed both similar water vapor transmission and moisture absorption as the control samples, while that applied at lower RH showed the highest hygric elongation, which was followed by those samples treated with the same product after conditioning at the higher RH. This suggests that the solvent based water repellent has the negative feature, similar to that of other conservation products, of increasing hygric and hydric elongation (Bachem and Littmann 2001). As the solvent formulation has a higher concentration of siloxane, this might also be a contributing factor. Overall, the water based water repellent appeared not to induce significant changes in any of the properties measured and has the advantage of not releasing volatile organic compounds thus being a more environmentally friendly product.

The answers to the original questions posed for this study are:

1. The water based SPD water repellent shows the same trend as observed for treatment of concrete. Samples conditioned at a lower RH adsorbed less moisture than those conditioned at higher RH, and furthermore, they appeared to adsorb less moisture than the controls, although there was no significant differences at a 95% confidence level.

2. The hygroscopic swelling of the sandstone was significantly modified by the solvent based NST water repellent while for the water based water repellent no significant difference was found with the control samples.

Bibliography

American Society for the Testing of Materials. "ASTM D421 − 85: Standard Practice for Dry Preparation of Soil Samples for Particle-Size Analysis and Determination of Soil Constants." *ASTM International*. 2007.

———."ASTM E96-10: Standard Test Methods for Water Vapor Transmission of Materials." *ASTM International*. 2011.

———."C490/C490M − 11: Standard Practice for use of Apparatus for the Determination of Length Change of Hardened Cement Paste, Mortar, and Concrete." *ASTM International*. 2010.

———."C948 – 81: Standard Test Method for Dry and Wet Bulk Density, Water Absorption, and Apparent Porosity of Thin Sections of Glass-Fiber Reinforced Concrete." *ASTM International*. 2009.

———."C97/C97M – 09: Standard Test Methods for Absorption and Bulk Specific Gravity of Dimension Stone." *ASTM International*. 2009.

———."D422 – 63: Standard Test Method for Particle-Size Analysis of Soils." *ASTM International*. 2007.

Arkles, B. "Tailoring Surfaces with Silanes." *Chemtech* 7 (1977): 766-778.

Bachem, A., and K. Littmann. "Selection of a Hydrophobic Polyurethane Material for the Restoration of a Wayside Shrine." *Hydrophobe III: 3rd International Conference on Surface Technology with Water Repellent Agents* (2001): 223-232.

Barshad, Isaac. "The Effect of the Interlayer Cations on the Expansion of the Mica Type of Crystal Lattice." *American Mineralogist* 35, no. 3-4 (1950): 225-238.

Bell, Michael. *The Face of Connecticut: People, Geology, and the Land*. State Geological and Natural History Survey of Connecticut, Dept. of Environmental Protection, 1985.

Biscontin, Guido, A. Bakolas, Elisabetta Zendri, and A. Moropoulou. "Interaction of some Protective Agents with Building Materials." *Methods of Evaluating Products for the Conservation of Porous Building Materials in Monuments: Preprints of the International Colloquium* (1995): 317-330.

Bowles, Oliver. *The Stone Industries*. McGraw-Hill Book Company, Inc., 1939.

Brown, G. and D. M. C. MacEwan. "The Interpretation of X-Ray Diagrams of Soil Clays. II. Structures with Random Interstratification." *Journal of Soil Science* 1, no. 2 (1950): 239-253.

Charola, A. E., J. Delgado Rodrigues, and M. Vale Anjos. "Disfiguring Biocolonization Patterns after the Application of Water Repellents." *Restoration of Buildings and Monuments* 14, no. 5 (2008): 365-372.

Charola, A. Elena. "Water Repellents and Other Protective Treatments: A Critical Review." *Hydrophobe III: 3rd International Conference on Surface Technology with Water Repellent Agents* (2001): 3-20.

———. "Water-Repellent Treatments for Building Stones: A Practical Overview." *APT Bulletin* 26 (1995): 10-17.

Charola, A. E., G. E. Wheeler, and G. G. Freund. "The Influence of Relative Humidity in the Polymerization of Methyl Trimethoxy Silane." In *Adhesives and Consolidants. Preprints of the Contributions to the IIC Paris Congress, 2-8 September 1984*, edited by Norman S. Brommelle, Elizabeth M. Pye, Perry Smith and Garry Thomson, 177-181. IIC: 1984.

Chiappone, Antonella, Stefania Marello, Claudio Scavia, and Massimo Setti. "Clay Mineral Characterization through the Methylene Blue Test: Comparison with Other Experimental Techniques and Applications of the Method." *Canadian Geotechnical Journal* 41(2004): 1168-1178.

Crosby, W. O., and G. F. Loughlin. "A Descriptive Catalogue of the Building Stones of Boston and Vicinity." *Technology Quarterly* 17 (1904): 165-185.

De Clercq, H. and E. De Witte. "Reactivity of Silicon Based Water Repellent Agents at Different Appliccation Conditions. Part I: Reactivity of Model Compounds." *Internationale Zeitschrift Für Bauinstandsetzen Und Baudenkmalpfege* 7, no. 1 (2001a): 63-78.

———."Reactivity of Silicon Based Water Repellent Agents at Different Appliccation Conditions. Part II: Commercial Water Repellents." *Internationale Zeitschrift Für Bauinstandsetzen Und Baudenkmalpfege* 7, no. 1 (2001b): 641-654.

De Witte, E., H. De Clercq, R. De Bruyn, and A. Pien. "Systematic Testing of Water Repellent Agents." In *Proceedings: First International Symposium on Surface Treatment of Building Materials with Water Repellent Agents, Delft University of Technology, Faculty of Architecture, Delft*, edited by F. H. Wittmann, A. J. M. Siemes and L. G. W. Verhoef, 5/1-5/10. 1995.

Fu, M. H., Z. Z. Zhang, and P. F. Low. " Changes in the Properties of a Montmorillonite-Water System during the Adsorption and Desorption of Water: Hysteresis." *Clays and Clay Minerals* 13, no. 5 (1990): 485-492.

Gerdes, A., and F. H. Wittmann. "Quality Control of Surface Treatments with Water Repellent Agents." In *Proceedings: First International Symposium on Surface Treatment of Building Materials with Water Repellent Agents, Delft University of Technology, Faculty of Architecture, Delft*, edited by F. H. Wittmann, Seinrn, H. A. A. J. and L. G. W. Verhoef, 15/1-15/7. 1995.

Glowacky, Jens, Stefan Heissler, Matthias Boese, Harald Leiste, Torsten Koker, Werner Faubel, Andreas Gerdes, and Harald S. Müller. 2008. "Investigation of Siloxane Film Formation of Functionalized Germanium Crystals by Atomic Microscopy and FTIR-ATR Spectroscopy." *Restoration of Building and Monuments* 14, no. 6 (2008): 413-424.

Goins, Elizabeth S., George Segan Wheeler, D. Griffiths, and Clifford A. Price. "The Effect of Sandstone, Limestone, Marble and Sodium Chloride on the Polymerization of MTMOS Solutions." In *Proceedings of the 8th International Congress on Deterioration and Conservation of Stone: Berlin, September 30th - October 4th, 1996*, edited by Joseph Riederer, 1243-1254. 1996.

Herb, H., G. Brenner-Weiß, and A. Gerdes. "TOF/MS for Characterization of Silicone Based Water Repellents." *Restoration of Building and Monuments* 14, no. 6 (2008): 395-402.

ICCROM. *ARC Laboratory Handbook*. Rome, Italy: International Center for the Study of the Preservation and Restoration of Cultural Property, 1999.

Jiménez González, Inmaculada, and George W. Scherer. "Effect of Swelling Inhibitors on the Swelling and Stress Relaxation of Clay Bearing Stones." *Environmental Geology* 46 (2004): 364-377.

———. "Evaluation the Potential Damage to Stones from Wetting and Drying Cycles." In *Measuring, Monitoring and Modeling Concrete Properties: An International Symposium Dedicated to Professor Surendra P. Shah, Northwestern University, U.S.A.*, edited by Maria S. Konsta-Gdoutos, 685-693. Springer, 2006.

Jiménez González, Inmaculada, Carlos Rodríguez-Navarro, and George W. Scherer. 2008. "Role of Clay Mineral in the Physicomechanical Deterioration of Sandstone." *Journal of Geophysical Research* 113 (2008): F02021.

Jiménez González, Inmaculada, Megan Higgins, and George W. Scherer. 2002. "Hygric Swelling of Portland Brownstone." Warrendale, PA, .

Jiménez González, Inmaculada, Robert Flatt, and Timothy Wangler. *Factors Affecting Portland Brownstone Durability: A Review*. LAP LAMBERT Academic Publishing, 2012.

Johansson, A., M. Janz, J. Silfwerbrand, and J. Trägårdh. "Penetration Depth for Water Repellent Agents in Concrete as a Function of Humidity, Porosity and Time." *Restoration of Building and Monuments* 13, no. 1 (2007): 3-16.

Johansson, Anders. *Impregnation of Concrete Structures -Transportation and Fixation of Moisture in Water Repellent Treated Concrete*. PHD dissertation, School of Architecture and the Built Environment at the Royal Institute of Technology (KTH), 2006.

Johansson, Anders, Mårten Janz, Jan Trägårdh, and Johan Silfwerbrand. "Sorption Isotherms of Water Repellent Treated Concrete." *Hydrophobe V: 5th International Conference on Water Repellent Treatment of Building Materials* (2008): 261-272.

Kober, Hermann. "Water-Thinnable Silicone Impregnating Agents for Masonty Protection." In *Proceedings: First International Symposium on Surface Treatment of Building Materials with Water Repellent Agents, Delft University of Technology, Faculty of Architecture, Delft*, edited by F. H. Wittmann, A. J. M. Siemes and L. G. W. Verhoef, 3/1-3/13. 1995.

Koblischek, Peter J. "Protection of Surfaces of Natural Stone and Concrete through Polymers." In *Proceedings: First International Symposium on Surface Treatment of Building Materials with Water Repellent Agents, Delft University of Technology, Faculty of Architecture, Delft*, edited by F. H. Wittmann, A. J. M. Siemes and L. G. W. Verhoef, 2/1-2/12. 1995.

Lewin, S. Z. and G. E. Wheeler. "Alkoxysilane Chemistry and Stone Conservation " In *Proceedings : Vth International Congress on Deterioration and Conservation of Stone*, 831-834. Lausanne, Suisse : Presses polytechniques romandes, 1985.

Manaresi, R. Rossi. "Stone Protection from Antiquity to the Beginning of the Industrial Revolution." *Science and Technology for Cultural Heritage: Journal of the "Comitato Nazionale Per La Scienza e La Tecnologia Dei Beni Culturali,"* CNR 2 (1993): 149-159.

Matero, Frank G., and Jeanne M. Teutonico. "The use of Architectural Sandstone in New York City in the 19th Century." *Bulletin of the Association for Preservation Technology* 14, no. 2 (1982): 11-17.

Moore, D. M. and R. C. Reynolds. *X-Ray Diffraction and the Identification and Analysis of Clay Minerals.* Oxford University Press, 1997.

Moreau, Claire, Ve´ronique Verge` s-Belmin, Lise Leroux, Genevie` ve Orial, Gilles Fronteau, and Vincent Barbin. "Water-Repellent and Biocide Treatments: Assessment of the Potential Combinations." *Journal of Cultural Heritage* 9 (2008): 394-400.

NORMAL. "Capillary Water Absorption and Capillary Absorption Coefficient." 11/85, 1985.

———. "Measurement of the Drying Index." 29/88, 1988.

Novich, Bruce E., and R. Torrence Martin. "Solvation Methods for Expandable Layers." *Clays and Clay Minerals* 31, no. 3 (1983): 235-238.

Oehmichen, D. S., A. Gerdes, and A. Wefer-Roehl. "Reactive Transport of Silanes in Cement Based Materials." *Restoration of Building and Monuments* 14, no. 6 (2008): 403-412.

Osterholtz, F. D., and E. R. Pohl. "Kinetics of the Hydrolysis and Condensation of Organofunctional Alkoxysilanes: A Review." *Journal of Adhesion Science and Technology* 6, no. 1 (1992): 127-149.

Pallatt, Nadia, Jeff Wilson, and Bill McHardy. "The Relationship between Permeability and the Morphology of Diagenetic Illite in Reservoir Rocks." *Journal of Petroleum Technology* 36, no. 12 (1984): 2225-2227.

Penati, A. "Protectives for Stone Materials: The Present State of the Art." *Science and Technology for Cultural Heritage : Journal of the "Comitato Nazionale Per La Scienza e La Tecnologia Dei Beni Culturali,"* CNR 2 (1993): 141-147.

Ruedrich, Joerg, Tobias Bartelsen, Reiner Dohrmann, and Siegfried Siegesmund. "Moisture Expansion as a Deterioration Factor for Sandstone used in Buildings." *Environmental Earth Sciences* 63, no. 7-8 (2010): 1545-1564.

Sasse, H. R. and R. Snethlage. "Methods for the Evaluation of Stone Conservation Treatments." Chap. 12, In *Saving our Architectural Heritage: The Conservation of Historic Stone Structure*, edited by N. S. Baer and R. Snethlage, 223-243. New York: John Wiley & Sons, 1997.

Scherer, George W. and Inmaculada Jiménez González. "Characterization of Swelling in Clay-Bearing Stone." *Geological Society of America Special Papers* 390 (2005): 51-61.

Seinrn, H. A. A. J. "Funcosil WS: Aqueous, Hydrophobizing Agent for Cementitious Building Materials." In *Proceedings: First International Symposium on Surface Treatment of Building Materials with Water Repellent Agents, Delft University of Technology, Faculty of Architecture, Delft*, edited by F. H. Wittmann, A. J. M. Siemes and L. G. W. Verhoef, 4/1-4/5. 1995.

Smith, David E. "Molecular Computer Simulations of the Swelling Properties and Interlayer Structure of Cesium Montmorillonite." *Langmuir* 14 (1998): 5959-5967.

Snethlage, R., and E. Wendler. "Moisture Cycles and Sandstone Degradation." In *Saving our Architectural Heritage: The Conservation of Historic Stone Structures*, edited by N. S.Baer and R. Snethlage, 7-24. New York: John Wiley & Sons, 1997.

Stapel, E. E., and P. N. W. Verhoef. "The use of the Methylene Blue Adsorption Test in Assessing the Quality of Basaltic Tuff Rock Aggregate." *Engineering Geology* 26 (1989): 233-246.

Steindlberger, Enno. "Volcanic Tuffs from Hesse (Germany) and their Weathering Behaviour." *Environmental Geology* 46 (2004): 378-390.

Tambach, Tim J., Peter G. Bolhuis, Emiel J. M. Hensen, and Berend Smit. "Hysteresis in Clay Swelling Induced by Hydrogen Bonding: Accurate Prediction of Swelling States." *Langmuir* 22 (2006): 1223-1234.

Tambach, Tim J., Emiel J. M. Hensen, and Berend Smit. "Molecular Simulations of Swelling Clay Minerals." *Journal of Physical Chemistry B* 108, no. 23 (2004): 7586-7596.

Teutonico, Jeanne Marie. *A Laboratory Manual for Architectural Conservators*. Rome: ICCROM, 1988.

Turkington, Alice V., and Thomas R. Paradise. "Sandstone Weathering: A Century of Research and Innovation." *Geomorphology* 67, no. 1-2 (2005): 229-253.

United States Census Office 10th census. *Report on the Building Stones of the United States, and Statistics of the Quarry Industry for 1880*. Washington, 1883.

van der Klugt, Loek J. A. R., and Jaap A. G. Koek. "The Effective use of Water-Repellents." In *Proceedings: First International Symposium on Surface Treatment of Building Materials with Water Repellent Agents, Delft University of Technology, Faculty of Architecture, Delft*, edited by F. H. Wittmann, A. J. M. Siemes and L. G. W. Verhoef, 19/1-19/4. 1995.

Van Hellemont, Y., H. De Clercq, and M. Van Bos. "Water Repellents and Anti-Graffiti : A Standard Safe Approach ?" *Hydrophobe V: 5th International Conference on Water Repellent Treatment of Building Materials* (2008): 145-154.

Wangler, Timothy, and George W. Scherer. "Clay Swelling Inhibition Mechanism of α,ω-Diaminoalkanes in Portland Brownstone." *Journal of Materials Research* 24, no. 5 (2009): 1646-1652.

———. "Clay Swelling Mechanism in Clay-Bearing Sandstones." *Environmental Geology* 56, no. 3-4 (2008): 529-534.

———. "Controlling Swelling of Portland Brownstone." *MRS Proceedings* 1047 (2007).

Weaver, Charles E. "The Distribution and Identification of Mixed-Layer Clays in Sedimentary Rocks." *American Mineralogist* 41 (1956): 202-221.

Weiss, T., S. Siegesmund, D. Kirchner, and J. Sippel. "Insolation Weathering and Hygric Dilatation: Two Competitive Factors in Stone Degradation." *Environmental Geology* 46 (2004): 402-413.

Worden, R. H., and S. Morad. "Clay Minerals in Sandstones: Control on Formation, Distribution and Evolution." *International Association of Sedimentologists Special Publication* 34 (2003): 3-41.

Young, J. F. "Humidity Control in the Laboratory using Salt Solutions—A Review." *Journal of Applied Chemistry* 17, no. 9 (1967): 241-245.

Appendix A. Sorption isotherms data

Table A.1 Drying weight of the prism assemblies to determine their initial dry weight.

Balance Sensitivity	0.01g															
Date	1/31/13	2/1/13	2/3/13	2/6/13	2/9/13	2/10/13	2/14/13	2/16/13	2/18/13	2/19/13	2/20/13	2/22/13	2/26/13	2/27/13	2/28/13	3/1/13
Oven T (°C)	60	60	60	60	60	60	60	60	60	60	60	60	110	60	60	60
Mass (g)																
SL1	240.63	240.30	240.30	240.32	240.29	240.26	240.32	240.28	240.27	240.31	240.28	240.27	240.20	240.22	240.24	240.25
SL2	224.37	224.07	224.07	224.09	224.05	224.04	224.09	224.03	224.03	224.06	224.03	224.03	223.97	224.00	224.02	224.01
SL3	211.46	211.18	211.18	211.21	211.17	211.15	211.20	211.15	211.15	211.18	211.16	211.14	211.10	211.12	211.13	211.14
NL1	190.78	190.54	190.54	190.57	190.52	190.51	190.55	190.50	190.50	190.54	190.52	190.50	190.46	190.49	190.51	190.50
NL2	217.50	217.22	217.22	217.24	217.20	217.19	217.24	217.19	217.17	217.22	217.20	217.18	217.12	217.15	217.17	217.17
NL3	199.36	199.10	199.10	199.12	199.09	199.07	199.11	199.09	199.06	199.10	199.08	199.07	199.02	199.04	199.05	199.06
CL1	220.37	220.07	220.07	220.09	220.06	220.03	220.09	220.05	220.04	220.06	220.05	220.04	219.96	219.99	220.01	220.01
CL2	214.29	214.00	214.01	214.04	213.99	213.99	214.03	213.98	213.96	214.01	214.00	213.97	213.91	213.94	213.96	213.96
CL3	202.62	202.36	202.36	202.38	202.34	202.33	202.39	202.33	202.31	202.36	202.34	202.32	202.27	202.30	202.31	202.31
SH1	220.21	219.93	219.93	219.95	219.91	219.89	219.95	219.90	219.89	219.92	219.90	219.89	219.83	219.85	219.87	219.88
SH2	190.68	190.42	190.42	190.44	190.41	190.39	190.45	190.40	190.39	190.42	190.41	190.39	190.34	190.36	190.38	190.37
SH3	206.13	205.86	205.86	205.88	205.85	205.85	205.89	205.85	205.84	205.87	205.85	205.83	205.77	205.80	205.82	205.81
NH1	211.18	210.91	210.91	210.94	210.90	210.88	210.94	210.89	210.87	210.91	210.89	210.88	210.82	210.84	210.86	210.86
NH2	201.35	201.10	201.10	201.12	201.09	201.06	201.12	201.07	201.06	201.09	201.06	201.06	201.01	201.04	201.05	201.04
NH3	209.86	209.58	209.58	209.60	209.56	209.55	209.60	209.55	209.55	209.58	209.55	209.55	209.47	209.51	209.52	209.52
CH1	220.75	220.45	220.46	220.48	220.44	220.42	220.47	220.42	220.41	220.46	220.44	220.42	220.35	220.37	220.40	220.40
CH2	199.42	199.16	199.16	199.18	199.15	199.13	199.18	199.14	199.13	199.17	199.15	199.14	199.10	199.11	199.13	199.13
CH3	212.53	212.25	212.25	212.27	212.24	212.21	212.28	212.23	212.22	212.25	212.23	212.22	212.15	212.18	212.20	212.19

Table A.2 Weight of the prism assemblies conditioned at 43 % RH and 75 % RH for moisture content before treatment application. The water repellent was applied on March 20th, 2013.

RH [L]	43 %				
RH [H]	75 %				
Balance Sensitivity	0.01 g				
Date	3/4/13	3/7/13	3/10/13	3/14/13	3/20/13
Mass (g)					
SL1	240.58	240.60	240.59	240.60	240.59
SL2	224.33	224.34	224.32	224.33	224.33
SL3	211.42	211.44	211.42	211.43	211.43
NL1	190.77	190.78	190.75	190.77	190.77
NL2	217.47	217.48	217.48	217.48	217.48
NL3	199.34	199.34	199.34	199.35	199.35
CL1	220.32	220.33	220.32	220.34	220.33
CL2	214.25	214.27	214.25	214.26	214.26
CL3	202.60	202.60	202.59	202.59/60	202.60
SH1	220.39	220.41	220.39	220.41	220.40
SH2	190.83	190.84	190.83	190.84	190.84
SH3	206.31	206.32	206.31	206.32	206.32
NH1	211.37	211.38	211.37	211.38	211.37
NH2	201.54	201.55	201.54	201.55	201.55
NH3	210.05	210.07	210.06	210.06	210.07
CH1	220.92	220.94	220.92	220.93/94	220.93
CH2	199.59	199.61	199.59	199.61	199.60
CH3	212.73	212.75	212.73	212.73	212.74

Table A.3 Drying weight of the prism assemblies to determine their dry weight after treatment application. The samples were put in oven on March 29th, 2013 and the conditioning process began immediately after they were out of oven on June 1st, 2013.

Balance Sensitivity	0.01 g															
Date	3/29/13	4/2/13	4/4/13	4/6/13	4/26/13	5/16/13	5/17/13	5/18/13	5/19/13	5/21/13	5/22/13	5/23/13	5/29/13	5/31/13	6/1/13
Oven T (°C)	Not in oven	60	60	60	60	60	60	60	60	60	60	60	60	60	60
Mass															
SL1	240.55	240.28	240.27	240.31	240.34	240.39	240.36	240.34	240.37	240.36	240.34	240.36	240.38	240.36	240.33
SL2	224.28	224.06	224.04	224.08	224.08	224.14	224.11	224.11	224.12	224.12	224.10	224.11	224.12	224.11	224.09
SL3	211.39	211.16	211.15	211.19	211.19	211.26	211.23	211.21	211.24	211.23	211.21	211.23	211.25	211.21	211.21
NL1	190.75	190.55	190.54	190.57	190.57	190.61	190.61	190.59	190.62	190.60	190.59	190.59	190.61	190.59	190.58
NL2	217.48	217.25	217.24	217.26	217.26	217.32	217.29	217.28	217.30	217.30	217.28	217.30	217.31	217.28	217.27
NL3	199.32	199.11	199.10	199.12	199.14	199.18	199.16	199.15	199.17	199.16	199.15	199.16	199.18	199.16	199.15
CL1	220.23	220.00	219.99	220.03	220.04	220.10	220.08	220.05	220.08	220.07	220.07	220.07	220.08	220.07	220.05
CL2	214.16	213.95	213.95	213.98	213.98	214.03	214.02	213.99	214.01	214.01	214.00	214.01	214.04	214.00	214.00
CL3	202.50	202.31	202.30	202.32	202.33	202.39	202.37	202.36	202.38	202.36	202.36	202.37	202.37	202.36	202.35
SH1	220.15	219.93	219.92	219.93	219.96	220.01	219.98	219.96	219.99	219.99	219.97	219.97	219.99	219.98	219.97
SH2	190.60	190.40	190.41	190.43	190.43	190.48	190.46	190.45	190.48	190.46	190.45	190.45	190.48	190.45	190.45
SH3	206.05	205.85	205.84	205.86	205.87	205.92	205.91	205.89	205.92	205.90	205.89	205.89	205.91	205.88	205.89
NH1	211.14	210.91	210.90	210.91	210.93	210.99	210.96	210.95	210.98	210.97	210.97	210.96	210.98	210.95	210.94
NH2	201.31	201.08	201.08	201.11	201.11	201.17	201.15	201.12	201.16	201.15	201.14	201.14	201.16	201.14	201.12
NH3	209.81	209.58	209.57	209.60	209.60	209.66	209.63	209.62	209.65	209.64	209.63	209.63	209.64	209.62	209.61
CH1	220.63	220.40	220.41	220.43	220.44	220.48	220.47	220.46	220.49	220.46	220.45	220.47	220.46	220.46	220.45
CH2	199.32	199.12	199.12	199.14	199.14	199.20	199.18	199.17	199.19	199.18	199.16	199.17	199.20	199.17	199.16
CH3	212.42	212.21	212.20	212.22	212.23	212.29	212.26	212.26	212.28	212.27	212.26	212.25	212.27	212.26	212.24

Table A.4 Weight of the prism assemblies conditioned at 43 % RH for sorption isotherms after treatment application.

Balance Sensitivity	0.01 g			
RH	43 %			
Date	6/5/13	6/9/13	6/12/13	6/15/13
Mass (g)				
SL1	240.64	240.66	240.63	240.63
SL2	224.37	224.39	224.36	224.36
SL3	211.46	211.47	211.45	211.46
NL1	190.81	190.83	190.80	190.81
NL2	217.54	217.56	217.53	217.53
NL3	199.38	199.40	199.38	199.38
CL1	220.34	220.35	220.33	220.33
CL2	214.27	214.29	214.26	214.25
CL3	202.60	202.62	202.60	202.59
SH1	220.23	220.26	220.22	220.22
SH2	190.68	190.69	190.67	190.67
SH3	206.14	206.17	206.13	206.13
NH1	211.21	211.22	211.20	211.2
NH2	201.38	201.39	201.37	201.37
NH3	209.87	209.90	209.87	209.87
CH1	220.73	220.75	220.72	220.73
CH2	199.42	199.44	199.41	199.41
CH3	212.52	212.54	212.52	212.51

Table A.5 Weight of the prism assemblies conditioned at 75 % RH for sorption isotherms after treatment application.

Balance Sensitivity	0.01 g			
RH	75 %			
Date	6/18/13	6/21/13	6/25/13	7/3/13
Mass (g)				
SL1	240.80	240.81	240.81	240.87
SL2	224.52	224.52	224.53	224.58
SL3	211.60	211.61	211.61	211.66
NL1	190.94	190.94	190.94	190.98
NL2	217.68	217.68	217.68	217.74
NL3	199.51	199.51	199.52	199.56
CL1	220.49	220.51	220.50	220.56
CL2	214.41	214.43	214.42	214.48
CL3	202.75	202.76	202.75	202.80
SH1	220.37	220.37	220.38	220.43
SH2	190.80	190.79	190.80	190.84
SH3	206.27	206.28	206.27	206.33
NH1	211.35	211.35	211.35	211.41
NH2	201.51	201.51	201.51	201.55
NH3	210.01	210.02	210.01	210.07
CH1	220.89	220.88	220.89	220.94
CH2	199.56	199.55	199.55	199.61
CH3	212.68	212.68	212.67	212.73

Table A.6 Weight of the prism assemblies conditioned at 98 % RH for sorption isotherms after treatment application.

Balance Sensitivity	0.01 g						
RH	98 %						
Date	7/9/13	7/14/13	7/17/13	7/23/13	7/26/13	7/29/13	8/1/13
Mass (g)							
SL1	240.88	241.27	241.30	241.39	241.45	241.44	241.48
SL2	224.59	225.00	225.13	225.26	225.33	225.32	225.34
SL3	211.67	212.03	212.14	212.25	212.30	212.29	212.31
NL1	190.99	191.46	191.52	191.67	191.68	191.70	191.70
NL2	217.75	218.20	218.25	218.46	218.45	218.49	218.48
NL3	199.56	200.05	200.16	200.39	200.41	200.42	200.43
CL1	220.57	221.08	221.25	221.40	221.47	221.45	221.46
CL2	214.50	214.96	214.95	215.08	215.08	215.12	215.11
CL3	202.82	203.23	203.19	203.30	203.32	203.33	203.34
SH1	220.44	220.91	220.94	221.11	221.12	221.12	221.13
SH2	190.86	191.30	191.38	191.60	191.59	191.63	191.63
SH3	206.34	206.76	206.77	206.93	206.92	206.95	206.94
NH1	211.42	211.75	211.83	211.92	211.95	211.95	211.99
NH2	201.56	201.91	201.96	202.05	202.09	202.09	202.11
NH3	210.08	210.55	210.56	210.75	210.72	210.76	210.74
CH1	220.95	221.51	221.68	221.86	221.92	221.91	221.92
CH2	199.62	200.27	200.37	200.55	200.57	200.57	200.60
CH3	212.74	213.24	213.32	213.45	213.48	213.49	213.52

Appendix B. Hygric linear expansion data

Table B.1 Length of the prism assemblies to determine their initial length.

Equipment Sensitivity	0.002 mm																			
Date	2/9/13	2/10/13	2/14/13		2/16/13		2/18/13		2/19/13		2/20/13		2/22/13		2/26/13		2/27/13		3/1/13	
Oven T (°C)	60	60	60		60		60		60		60		60		110		60		60	
Length Reading (mm)				**Min**		**Min**		**Min**		**Min**		**Min**		**Min**		**Min**		**Min**		**Min**
SL1	-0.288	-0.294	-0.294	-0.294	-0.298	-0.330	-0.298	-0.330	-0.298	-0.330	-0.298	-0.330	-0.298	-0.326	-0.298	-0.330	-0.298	-0.326	-0.302	-0.332
SL2	0.072	0.072	0.076	-0.004	0.078	-0.004	0.070	-0.010	0.070	-0.010	0.068	-0.012	0.070	-0.010	0.076	-0.004	0.076	-0.006	0.072	-0.010
SL3	-0.132	-0.136	-0.134	-0.136	-0.132	-0.134	-0.136	-0.138	-0.136	-0.138	-0.138	-0.142	-0.136	-0.138	-0.136	-0.138	-0.136	-0.138	-0.136	-0.138
NL1	0.012	0.012	0.016	-0.048	0.016	-0.044	0.014	-0.050	0.010	-0.050	0.006	-0.054	0.012	-0.048	0.012	-0.050	0.012	-0.050	0.012	-0.050
NL2	-0.134	-0.138	-0.144	-0.296	-0.138	-0.292	-0.132	-0.296	-0.126	-0.294	-0.126	-0.296	-0.126	-0.294	-0.110	-0.292	-0.118	-0.294	-0.126	-0.292
NL3	-0.032	-0.038	-0.044	-0.058	-0.044	-0.058	-0.042	-0.060	-0.042	-0.060	-0.044	-0.060	-0.040	-0.058	-0.042	-0.058	-0.042	-0.058	-0.044	-0.060
CL1	0.012	0.006	0.006	-0.042	0.006	-0.044	0.006	-0.044	0.006	-0.048	0.006	-0.048	0.010	-0.044	0.012	-0.044	0.010	-0.044	0.010	-0.044
CL2	0.072	0.072	0.076	0.044	0.076	0.042	0.070	0.040	0.070	0.038	0.068	0.038	0.070	0.040	0.068	0.038	0.066	0.038	0.066	0.034
CL3	0.454	0.454	0.456	0.372	0.456	0.364	0.452	0.362	0.452	0.362	0.448	0.362	0.448	0.362	0.452	0.364	0.452	0.364	0.452	0.364
SH1	0.370	0.370	0.374	0.368	0.372	0.364	0.368	0.360	0.370	0.360	0.370	0.362	0.372	0.364	0.372	0.362	0.372	0.362	0.370	0.360
SH2	0.044	0.038	0.042	0.004	0.038	0.002	0.038	0.000	0.038	0.002	0.038	0.002	0.038	0.002			0.042	0.010	0.042	0.010
SH3	0.022	0.020	0.020	-0.032	0.020	-0.034	0.016	-0.040	0.016	-0.038	0.016	-0.038	0.020	-0.034	0.016	-0.038	0.020	-0.034	0.016	-0.040
NH1	-0.058	-0.054	-0.052	-0.052	-0.052	-0.052	-0.058	-0.058	-0.060	-0.060	-0.060	-0.060	-0.060	-0.060	-0.060	-0.060	-0.058	-0.060	-0.062	-0.062
NH2	-0.504	-0.504	-0.502	-0.520	-0.504	-0.522	-0.510	-0.528	-0.510	-0.528	-0.510	-0.524	-0.508	-0.524	-0.502	-0.522	-0.504	-0.522	-0.504	-0.524
NH3	0.762	0.758	0.762	0.702	0.758	0.700	0.758	0.694	0.758	0.698	0.756	0.698	0.756	0.698	0.756	0.698	0.756	0.698	0.756	0.698
CH1	-0.382	-0.382	-0.380	-0.392	-0.378	-0.390	-0.386	-0.396	-0.380	-0.398	-0.380	-0.398	-0.380	-0.398	-0.380	-0.396	-0.378	-0.396	-0.380	-0.396
CH2	-0.048	-0.052	-0.052	-0.098	-0.052	-0.098	-0.058	-0.104	-0.058	-0.104	-0.060	-0.106	-0.058	-0.100	-0.060	-0.100	-0.058	-0.098	-0.060	-0.100
CH3	-0.312	-0.320	-0.316	-0.390	-0.320	-0.392	-0.248	-0.396	-0.322	-0.396	-0.320	-0.396	-0.320	-0.392	-0.316	-0.390	-0.316	-0.392	-0.316	-0.392

Table B.2 Length of the prism assemblies conditioned at 43 % RH and 75 % RH for moisture content before treatment application. The water repellent was applied on March 20th, 2013.

RH [L]	43 %											
RH [H]	75 %											
Equipment Sensitivity	0.002 mm											
Date	3/1/13		3/4/13		3/7/13		3/10/13		3/14/13		3/20/13	
Length Reading (mm)		Min		Min		Min		Min		Min		Min
SL1	-0.302	-0.332	-0.296	-0.324	-0.294	-0.322	-0.294	-0.322	-0.294	-0.324	-0.294	-0.322
SL2	0.072	-0.010	0.076	-0.006	0.078	-0.002	0.080	0.000	0.078	-0.002	0.078	-0.002
SL3	-0.136	-0.138	-0.134	-0.134	-0.128	-0.134	-0.128	-0.132	-0.128	-0.132	-0.128	-0.132
NL1	0.012	-0.050	0.014	-0.048	0.014	-0.048	0.016	-0.042	0.016	-0.044	0.016	-0.042
NL2	-0.126	-0.292	-0.124	-0.288	-0.124	-0.288	-0.120	-0.286	-0.120	-0.286	-0.120	-0.286
NL3	-0.044	-0.060	-0.040	-0.054	-0.038	-0.054	-0.038	-0.052	-0.034	-0.052	-0.034	-0.052
CL1	0.010	-0.044	0.012	-0.042	0.012	-0.040	0.014	-0.040	0.016	-0.040	0.016	-0.038
CL2	0.066	0.034	0.068	0.038	0.068	0.042	0.068	0.042	0.068	0.042	0.068	0.042
CL3	0.452	0.364	0.454	0.368	0.456	0.370	0.456	0.370	0.456	0.372	0.458	0.372
SH1	0.370	0.360	0.378	0.368	0.382	0.372	0.382	0.374	0.382	0.374	0.382	0.372
SH2	0.042	0.010	0.048	0.014	0.052	0.016	0.052	0.020	0.052	0.020	0.052	0.016
SH3	0.016	-0.040	0.022	-0.032	0.026	-0.026	0.030	-0.026	0.026	-0.030	0.030	-0.026
NH1	-0.062	-0.062	-0.052	-0.054	-0.050	-0.050	-0.050	-0.050	-0.050	-0.050	-0.050	-0.050
NH2	-0.504	-0.524	-0.500	-0.520	-0.494	-0.514	-0.494	-0.514	-0.496	-0.514	-0.494	-0.514
NH3	0.756	0.698	0.762	0.706	0.766	0.708	0.766	0.708	0.766	0.708	0.768	0.710
CH1	-0.380	-0.396	-0.370	-0.388	-0.368	-0.386	-0.368	-0.386	-0.368	-0.386	-0.368	-0.386
CH2	-0.060	-0.100	-0.052	-0.092	-0.050	-0.090	-0.050	-0.090	-0.050	-0.090	-0.050	-0.090
CH3	-0.316	-0.392	-0.308	-0.386	-0.306	-0.380	-0.304	-0.380	-0.306	-0.382	-0.306	-0.380

Table B.3 Length of the prism assemblies to determine their length after treatment application. The samples were put in oven on March 29th, 2013 and the conditioning process began immediately after they were out of oven on June 1st, 2013.

Equipment Sensitivity	0.002 mm											
Date	3/29/13		5/21/13		5/22/13		5/23/13		5/31/13		6/1/13	
Oven T (°C)	Not in Oven		60		60		60		60		60	
Length Reading (mm)		Min		Min		Min		Min		Min		Min
SL1	-0.298	-0.324	-0.296	-0.320	-0.294	-0.322	-0.294	-0.322	-0.296	-0.322	-0.294	-0.320
SL2	0.066	-0.006	0.072	-0.002	0.070	-0.002	0.070	-0.002	0.070	-0.002	0.072	0.002
SL3	-0.116	-0.134	-0.116	-0.132	-0.116	-0.128	-0.116	-0.132	-0.116	-0.132	-0.116	-0.128
NL1	0.002	-0.044	0.002	-0.042	0.002	-0.042	0.002	-0.042	-0.002	-0.042	0.000	-0.040
NL2	-0.136	-0.288	-0.134	-0.292	-0.142	-0.288	-0.148	-0.286	-0.148	-0.288	-0.152	-0.284
NL3	-0.022	-0.052	-0.020	-0.052	-0.016	-0.050	-0.016	-0.050	-0.020	-0.050	-0.014	-0.048
CL1	0.034	-0.042	0.032	-0.038	0.032	-0.038	0.032	-0.040	0.030	-0.038	0.032	-0.034
CL2	0.040	0.040	0.040	0.040	0.042	0.042	0.042	0.042	0.042	0.040	0.048	0.048
CL3	0.420	0.368	0.424	0.370	0.426	0.372	0.424	0.370	0.420	0.368	0.426	0.374
SH1	0.380	0.362	0.382	0.364	0.386	0.370	0.386	0.368	0.386	0.370	0.388	0.370
SH2	0.040	0.010	0.048	0.014	0.048	0.014	0.044	0.012	0.044	0.012	0.048	0.016
SH3	0.034	-0.038	0.038	-0.032	0.038	-0.032	0.038	-0.032	0.038	-0.032	0.040	-0.026
NH1	-0.042	-0.054	-0.038	-0.054	-0.038	-0.054	-0.038	-0.054	-0.040	-0.058	-0.038	-0.054
NH2	-0.504	-0.522	-0.502	-0.518	-0.502	-0.518	-0.502	-0.520	-0.502	-0.520	-0.500	-0.518
NH3	0.766	0.702	0.766	0.706	0.768	0.706	0.766	0.706	0.764	0.706	0.768	0.710
CH1	-0.352	-0.396	-0.350	-0.390	-0.346	-0.390	-0.346	-0.390	-0.350	-0.388	-0.346	-0.386
CH2	-0.066	-0.098	-0.062	-0.096	-0.062	-0.096	-0.062	-0.096	-0.066	-0.096	-0.062	-0.092
CH3	-0.316	-0.388	-0.314	-0.386	-0.314	-0.382	-0.314	-0.382	-0.316	-0.382	-0.314	-0.380

Table B.4 Length of the prism assemblies conditioned at 43 % RH for sorption isotherms after treatment application.

RH	43 %							
Equipment Sensitivity	0.002 mm							
Date	6/5/13		6/9/13		6/12/13		6/15/13	
Length Reading (mm)		Min		Min		Min		Min
SL1	-0.292	-0.320	-0.292	-0.316	-0.288	-0.316	-0.292	-0.316
SL2	0.076	0.004	0.076	0.004	0.076	0.006	0.076	0.006
SL3	-0.110	-0.124	-0.110	-0.124	-0.110	-0.124	-0.110	-0.124
NL1	0.002	-0.034	0.002	-0.034	0.004	-0.034	0.004	-0.034
NL2	-0.152	-0.284	-0.152	-0.280	-0.146	-0.278	-0.152	-0.280
NL3	-0.014	-0.044	-0.014	-0.044	-0.012	-0.042	-0.014	-0.042
CL1	0.032	-0.032	0.034	-0.032	0.034	-0.032	0.034	-0.032
CL2	0.048	0.048	0.050	0.048	0.050	0.048	0.048	0.048
CL3	0.428	0.374	0.428	0.374	0.430	0.374	0.428	0.374
SH1	0.388	0.372	0.388	0.372	0.390	0.372	0.390	0.374
SH2	0.050	0.016	0.050	0.020	0.052	0.020	0.052	0.020
SH3	0.040	-0.026	0.040	-0.026	0.042	-0.024	0.042	-0.024
NH1	-0.034	-0.052	-0.034	-0.050	-0.032	-0.048	-0.032	-0.048
NH2	-0.496	-0.514	-0.496	-0.514	-0.496	-0.512	-0.496	-0.512
NH3	0.768	0.710	0.772	0.712	0.772	0.712	0.772	0.712
CH1	-0.344	-0.382	-0.344	-0.382	-0.344	-0.380	-0.346	-0.380
CH2	-0.060	-0.090	-0.060	-0.092	-0.058	-0.090	-0.060	-0.090
CH3	-0.312	-0.372	-0.312	-0.374	-0.308	-0.374	-0.312	-0.374

Table B.5 Length of the prism assemblies conditioned at 75 % RH for sorption isotherms after treatment application.

RH	75 %							
Equipment Sensitivity	0.002 mm							
Date	6/18/13		6/21/13		6/25/13		7/3/13	
Length Reading (mm)		Min		Min		Min		Min
SL1	-0.278	-0.304	-0.284	-0.312	-0.274	-0.302	-0.284	-0.308
SL2	0.088	0.020	0.080	0.012	0.090	0.022	0.080	0.010
SL3	-0.100	-0.114	-0.106	-0.118	-0.096	-0.108	-0.106	-0.118
NL1	0.020	-0.020	0.012	-0.026	0.020	-0.016	0.012	-0.026
NL2	-0.142	-0.268	-0.148	-0.274	-0.136	-0.264	-0.148	-0.270
NL3	-0.002	-0.030	-0.006	-0.038	0.000	-0.026	-0.006	-0.034
CL1	0.044	-0.020	0.040	-0.026	0.050	-0.016	0.040	-0.024
CL2	0.062	0.060	0.058	0.054	0.068	0.066	0.058	0.054
CL3	0.440	0.392	0.436	0.380	0.446	0.392	0.436	0.382
SH1	0.400	0.386	0.396	0.382	0.406	0.392	0.396	0.382
SH2	0.062	0.030	0.054	0.024	0.068	0.034	0.054	0.024
SH3	0.052	-0.012	0.048	-0.020	0.058	-0.010	0.048	-0.016
NH1	-0.020	-0.038	-0.026	-0.042	-0.014	-0.032	-0.024	-0.042
NH2	-0.486	-0.502	-0.490	-0.508	-0.482	-0.496	-0.492	-0.508
NH3	0.782	0.726	0.776	0.720	0.786	0.730	0.776	0.722
CH1	-0.334	-0.370	-0.340	-0.374	-0.332	-0.364	-0.340	-0.372
CH2	-0.050	-0.080	-0.054	-0.086	-0.044	-0.076	-0.052	-0.086
CH3	-0.302	-0.364	-0.304	-0.364	-0.296	-0.360	-0.306	-0.370

Table B.6 Length of the prism assemblies conditioned at 98 % RH for sorption isotherms after treatment application.

RH	98 %													
Equipment Sensitivity	0.002 mm													
Date	7/9/13		7/14/13		7/17/13		7/23/13		7/26/13		7/29/13		8/1/13	
Length Reading (mm)		Min		Min		Min		Min		Min		Min		Min
SL1	-0.284	-0.308	-0.280	-0.304	-0.276	-0.302	-0.274	-0.298	-0.274	-0.302	-0.276	-0.302	-0.274	-0.302
SL2	0.080	0.012	0.088	0.022	0.090	0.022	0.096	0.026	0.096	0.026	0.092	0.024	0.096	0.024
SL3	-0.104	-0.116	-0.098	-0.110	-0.092	-0.108	-0.092	-0.106	-0.092	-0.106	-0.096	-0.108	-0.092	-0.106
NL1	0.012	-0.026	0.020	-0.016	0.022	-0.012	0.026	-0.010	0.026	-0.010	0.024	-0.012	0.026	-0.010
NL2	-0.148	-0.274	-0.142	-0.266	-0.136	-0.264	-0.134	-0.258	-0.136	-0.260	-0.134	-0.258	-0.136	-0.260
NL3	-0.006	-0.038	0.000	-0.026	0.004	-0.024	0.010	-0.020	0.010	-0.020	0.006	-0.022	0.010	-0.020
CL1	0.040	-0.024	0.044	-0.014	0.050	-0.016	0.054	-0.012	0.052	-0.012	0.050	-0.014	0.052	-0.014
CL2	0.062	0.058	0.070	0.066	0.068	0.066	0.070	0.068	0.068	0.066	0.068	0.066	0.068	0.066
CL3	0.436	0.382	0.444	0.390	0.444	0.390	0.446	0.392	0.446	0.392	0.444	0.392	0.444	0.390
SH1	0.398	0.380	0.402	0.388	0.406	0.390	0.410	0.392	0.408	0.392	0.408	0.392	0.408	0.392
SH2	0.058	0.024	0.062	0.032	0.068	0.040	0.070	0.040	0.070	0.040	0.070	0.040	0.070	0.040
SH3	0.050	-0.016	0.054	-0.010	0.058	-0.006	0.062	-0.002	0.060	-0.006	0.060	-0.004	0.060	-0.006
NH1	-0.022	-0.038	-0.020	-0.030	-0.016	-0.032	-0.012	-0.030	-0.014	-0.030	-0.014	-0.030	-0.012	-0.030
NH2	-0.492	-0.508	-0.486	-0.502	-0.484	-0.496	-0.480	-0.494	-0.482	-0.494	-0.482	-0.496	-0.482	-0.494
NH3	0.776	0.722	0.784	0.730	0.786	0.734	0.792	0.736	0.788	0.734	0.788	0.734	0.788	0.734
CH1	-0.340	-0.372	-0.332	-0.364	-0.324	-0.362	-0.324	-0.358	-0.324	-0.360	-0.326	-0.360	-0.324	-0.360
CH2	-0.052	-0.086	-0.044	-0.078	-0.040	-0.072	-0.038	-0.070	-0.038	-0.070	-0.038	-0.070	-0.038	-0.070
CH3	-0.306	-0.368	-0.302	-0.362	-0.296	-0.358	-0.294	-0.354	-0.294	-0.352	-0.296	-0.358	-0.296	-0.354

Appendix C. Water vapor transmission data

Table C.1 Data of water vapor transmission test using the water method.

ELAPSED TIME (h)	SL1	SL2	SL3	NL1	NL2	NL3	CL2	CH1	DUMMY
0.00	123.05	123.77	125.83	127.82	124.44	122.19	119.37	121.63	101.41
1.00	123.04	123.77	125.82	127.81	124.44	122.19	119.37	121.63	101.39
4.25	123.04	123.75	125.82	127.81	124.43	122.19	119.37	121.62	101.39
26.50	123.01	123.74	125.79	127.79	124.40	122.16	119.34	121.58	101.37
47.08	122.97	123.73	125.78	127.78	124.39	122.14	119.30	121.55	101.37
74.83	122.92	123.70	125.75	127.75	124.36	122.10	119.25	121.51	101.37
99.70	122.86	123.67	125.71	127.73	124.32	122.06	119.20	121.45	101.36
118.75	122.82	123.65	125.69	127.70	124.30	122.03	119.17	121.42	101.37
143.92	122.79	123.62	125.67	127.68	124.27	122.01	119.13	121.39	101.37
169.78	122.73	123.59	125.62	127.65	124.23	121.96	119.08	121.33	101.37
208.50	122.63	123.51	125.54	127.57	124.15	121.87	118.98	121.23	101.36
232.22	122.54	123.46	125.48	127.52	124.09	121.81	118.91	121.16	101.35
257.37	122.47	123.42	125.44	127.48	124.03	121.75	118.82	121.09	101.36

Table C.2 Data of water vapor transmission test using the water method. Test was restarted when the sealing material broke up.

ELAPSED TIME (h)	SH2	SH3	NH1	NH2	NH3	CH3	ELAPSED TIME (h)	SH1
0.00	126.52	125.19	125.07	125.09	122.93	129.28	0.00	124.09
1.00	126.52	125.19	125.07	125.08	122.93	129.27	1.00	124.08
4.25	126.51	125.18	125.06	125.07	122.93	129.27	4.25	124.08
26.50	126.48	125.16	125.04	125.02	122.89	129.23	26.50	124.05
47.08	126.45	125.14	125.01	124.97	122.87	129.20	47.08	124.02
74.83	126.41	125.10	124.96	124.90	122.83	129.16	74.83	123.97
99.70	126.36	125.07	124.93	124.84	122.79	129.12	99.70	123.92
118.75	126.34	125.04	124.89	124.79	122.76	129.09	RESTART	
143.92	126.30	125.01	124.86	124.74	122.72	129.05	0.00	123.71
169.78	126.22	124.97	124.80	124.66	122.66	128.99	25.83	123.68
RESTART							64.08	123.60
0.00	125.89	124.79	124.56	124.54	122.65	129.15	87.80	123.54
38.25	125.79	124.71	124.48	124.47	122.57	129.05	112.95	123.49
61.97	125.73	124.66	124.42	124.43	122.51	129.00		
87.12	125.67	124.60	124.38	124.39	122.46	128.94		

Appendix D. Water absorption and drying curves data

Table D.1 Weight over time during capillary absorption

CUMULATIVE TIME t(s)	A (parallel)	B (parallel)	C (perpendicular)	D (perpendicular)
0	345.37	334.86	351.2	325.05
180	345.65	335.19	351.69	325.56
360	345.74	335.29	351.73	325.61
540	345.79	335.33	351.82	325.7
720	345.82	335.38	351.9	325.77
900	345.86	335.42	351.93	325.82
1080	345.89	335.46	351.99	325.87
1260	345.93	335.5	352.04	325.92
1440	345.96	335.53	352.09	325.98
1620	345.99	335.56	352.12	326.01
1800	346.02	335.59	352.17	326.06
1500	346.06	335.64	352.23	326.13
2400	346.11	335.68	352.29	326.18
2700	346.14	335.73	352.35	326.24
3000	346.18	335.76	352.39	326.29
3300	346.22	335.8	352.45	326.34
3600	346.25	335.83	352.48	326.38
4500	346.36	335.93	352.63	326.51
5400	346.45	336.03	352.75	326.64
7200	346.61	336.18	352.95	326.84
9000	346.75	336.33	353.14	327.03
10800	346.89	336.46	353.31	327.19
12600	347.01	336.58	353.46	327.35
16200	347.24	336.81	353.76	327.64
19020	347.39	336.95	353.96	327.83
31800	347.96	337.49	354.72	328.6
78000	349.54	339.01	356.78	330.65
91800	349.87	339.28	357.26	331.08
103620	350.02	339.45	357.56	331.39
116820	350.26	339.74	357.93	331.73
165480	351.22	340.71	359.18	332.88
196920	351.67	341.17	359.73	333.31
247800	352.63	342.08	360.46	333.66
269640	352.92	342.37	360.49	333.66
284400	353.14	342.56	360.54	333.69
332040	353.72	343.1	360.61	333.75
370800	354.03	343.41	360.64	333.77
425520	354.38	343.76	360.71	333.83
460500	354.43	343.76	360.69	333.82
529680	354.66	344.03	360.76	333.87
619500	354.76	344.17	360.83	333.93
686580	354.76	344.17	360.82	333.92
712680	354.8	344.21	360.86	333.95

CUMULATIVE TIME t(s)	A (parallel)	B (parallel)	C (perpendicular)	D (perpendicular)
765060	354.85	344.25	360.88	333.98
852600	354.78	344.18	360.81	333.92

Table D.2 Weight over time during drying

CUMULATIVE TIME t(h)	A (parallel)	B (parallel)	C (perpendicular)	D (perpendicular)
0.00	355.10	344.57	361.15	334.30
0.05	354.96	344.43	361.04	334.21
0.07	354.92	344.38	361.00	334.17
0.08	354.89	344.35	360.97	334.13
0.10	354.86	344.32	360.93	334.10
0.12	354.82	344.29	360.90	334.06
0.15	354.77	344.23	360.84	334.00
0.18	354.72	344.17	360.78	333.94
0.22	354.66	344.12	360.72	333.88
0.25	354.61	344.06	360.68	333.82
0.28	354.56	344.01	360.61	333.77
0.33	354.47	343.93	360.53	333.69
0.38	354.39	343.85	360.46	333.61
0.43	354.33	343.78	360.39	333.55
0.48	354.26	343.72	360.34	333.48
0.53	354.20	343.66	360.27	333.43
0.62	354.10	343.56	360.17	333.33
0.70	354.01	343.46	360.09	333.24
0.78	353.91	343.37	359.99	333.15
0.87	353.81	343.29	359.90	333.06
0.95	353.73	343.19	359.81	332.97
1.03	353.64	343.10	359.72	332.89
1.20	353.46	342.92	359.55	332.71
1.28	353.37	342.83	359.46	332.62
1.37	353.28	342.74	359.38	332.54
1.53	353.11	342.57	359.21	332.37
1.78	352.86	342.33	358.96	332.14
2.03	352.63	342.10	358.73	331.91
2.33	352.36	341.82	358.46	331.65
2.70	352.06	341.50	358.15	331.35
3.03	351.80	341.24	357.90	331.08
3.62	351.41	340.84	357.50	330.71
4.03	351.18	340.59	357.26	330.46
5.07	350.66	340.04	356.71	329.96
6.78	350.09	339.46	356.12	329.41
8.03	349.79	339.15	355.81	329.13
10.13	349.43	338.78	355.43	328.78
25.43	348.27	337.63	354.21	327.68

CUMULATIVE TIME t(h)	A (parallel)	B (parallel)	C (perpendicular)	D (perpendicular)
33.87	347.96	337.33	353.88	327.39
52.95	347.53	336.90	353.43	326.99
59.17	347.39	336.78	353.29	326.87
72.50	347.25	336.64	353.14	326.75
81.95	347.21	336.61	353.10	326.71
98.70	347.13	336.52	353.01	326.65
120.67	347.01	336.42	352.89	326.55
127.15	346.97	336.38	352.85	326.51
152.30	346.89	336.32	352.77	326.45

Appendix E. PROSOCO water repellent data sheet

E.1 Sure Klean® Weather Seal Natural Stone Treatment Water Repellent Specification

Specifier Note: The information provided below is intended to guide the Architect in developing specifications for products manufactured by PROSOCO, Inc. and should not be viewed as a complete source of information about the product(s). The Architect should always refer to the Product Data Sheet and MSDS for additional recommendations and for safety information

Specifier Note: Paragraph below is for PART 1 GENERAL, Quality Assurance.

Test Area
Test a minimum 4 ft. by 4 ft. area on each type of masonry. Use the manufacturer's application instructions. Let test area protective treatment cure before inspection. Keep test panels available for comparison throughout the protective treatment project.

Specifier Note: Paragraphs below are for PART 2 PRODUCTS, Manufacturers and Products.

Manufacturer: PROSOCO, Inc., 3741 Greenway Circle, Lawrence, KS 66046. Phone: (800) 255-4255; Fax: (785) 830-9797. E-mail: CustomerCare@prosoco.com

Product Description
Sure Klean® Weather Seal Natural Stone Treatment is a modified siloxane water repellent developed for limestone, marble and most other traditional masonry surfaces. Natural Stone Treatment penetrates deeply to provide long-lasting protection without altering the natural appearance of the substrate.

Natural Stone Treatment is modified for effectiveness on most limestone, marble and other calcareous surfaces to provide water repellent protection superior to more common silane, siloxane, acrylic or metallic stearate water repellents. Natural Stone Treatment reduces the severity of biological staining common to regions with high relative humidity. Treated surfaces resist dark staining and degradation caused by fungal growth, mold and mildew.

Typical Technical Data

FORM: Clear liquid, mild odor
SPECIFIC GRAVITY: 0.805
pH: not applicable
WEIGHT/GALLON: 6.70 pounds
ACTIVE CONTENT: 11 percent
TOTAL SOLIDS: 9 percent ASTM D 5095
FLASH POINT: 118 degrees F (48 degrees C) ASTM D 3278
FREEZE POINT: less than -22 degrees F (less than -30 degrees C)
SHELF LIFE: 2 years in tightly sealed, unopened container
VOC CONTENT: Manufactured and marketed in compliance with USEPA AIM VOC regulations (40 CFR 59.403). Not suitable for sale in states and districts with more restrictive AIM VOC regulations.

Limitations

- May damage glass or be difficult to remove. Always protect.
- Not appropriate for application to asphaltic or painted surfaces.
- Not suitable for application to synthetic resin paints, gypsum, plaster or other non-masonry surfaces.
- Not recommended for below-grade application.
- Will not prevent water penetration through structural cracks, defects, open joints or material defects.

Specifier Note: Paragraphs below are for PART 3 EXECUTION, Installation.

Application

Before applying, read “Preparation” and “Safety Information” sections in the Manufacturer’s Product Data Sheet for Weather Seal Natural Stone Treatment. Refer to the Product Data Sheet for additional information about application of Weather Seal Natural Stone Treatment. Apply as packaged. Do not alter or dilute.

Vertical Application Instructions

For best results, apply protective treatment “wet-on-wet” to a thoroughly dry surface from the bottom up. For spray applications, use enough material to create a 6 to 8 inch rundown below the spray contact point. Let the first application penetrate the masonry surface and then reapply (within 5 minutes) in the same saturating manner. Less material will be required on the second application.

SPECIFIER NOTE: when using a brush, roller or lamb's wool applicator, saturate the surface. Brush out heavy runs and drips that do not penetrate after a few minutes.

Horizontal Application Instructions
Apply a single saturating application using enough to keep the surface wet for a few minutes. Thoroughly broom out puddles that do not completely penetrate the surface. Soak up any remaining material with a clean towel.

Dense Surface Application Instructions
Apply a single coat using enough to completely wet the surface without creating drips, puddles or rundown. Do not over apply.

Drying Time: Protect treated surfaces from rain and pedestrian traffic for 4 to 6 hours following application. Product gains its water repellency properties in 72 hours.

Cleanup: clean tools and equipment immediately with mineral spirits or and equivalent cleaning solvent. Remove over spray and spills as soon as possible.

E.2 Sure Klean® Weather Seal Siloxane PD Water Repellent Specification

Specifier Note: The information provided below is intended to guide the Architect in developing specifications for products manufactured by PROSOCO, Inc. and should not be viewed as a complete source of information about the product(s). The Architect should always refer to the Product Data Sheet and MSDS for additional recommendations and for safety information.

Specifier Note: Paragraph below is for PART 1 GENERAL, Quality Assurance.

Test Area
Test a minimum 4 ft. by 4 ft. area on each type of masonry. Use the manufacturer's application instructions. Let test area protective treatment cure before inspection. Keep test panels available for comparison throughout the protective treatment project.

Specifier Note: Paragraphs below are for PART 2 PRODUCTS, Manufacturers and Products.

Manufacturer: PROSOCO, Inc., 3741 Greenway Circle, Lawrence, KS 66046. Phone: (800) 255-4255; Fax: (785) 830-9797. E-mail: CustomerCare@prosoco.com

Product Description
Sure Klean® Weather Seal Siloxane PD (predilute) is a ready to-use, water-based silane/siloxane water repellent for concrete and most masonry and stucco surfaces. Siloxane PD is a low-VOC treatment that penetrates more deeply than conventional water repellents and helps masonry resist cracking, spalling, staining and other damage related to water intrusion. Low odor and alkaline stable, Siloxane PD is ideal for field and in-plant application.

Technical Data
FORM: White milky liquid
SPECIFIC GRAVITY: 0.996
ACTIVE CONTENT: 7%
pH: 4-5
WT./GAL.: 8.29 lbs.
FLASH POINT: > 212 degrees F (> 100 degrees C) ASTM D 3278
FREEZE POINT: 32 degrees F (0 degrees C)
VOC CONTENT: Complies with all known national, state and district AIM VOC regulations.

Limitations
- Won't keep water out of cracks, defects or open joints.
- Not recommended for below grade application..

Specifier Note: Paragraphs below are for PART 3 EXECUTION, Installation.

Application
Before applying, read "Preparation" and "Safety Information" sections in the Manufacturer's Product Data Sheet for Weather Seal Siloxane PD. Refer to the Product Data Sheet for additional information about application of Weather Seal Siloxane PD. Do not dilute or alter.

Vertical Application Instructions
For best results, apply protective treatment "wet-on-wet" to a visibly dry and absorbent surface.

Spray: Saturate from the bottom up, creating a 4" to 8" (15 to 20 cm) rundown below the spray contact point. Let the first application penetrate for 5-10 minutes. Resaturate. Less will be needed for the second application.

Brush or roller: Saturate uniformly. Let protective treatment penetrate for 5 to 10 minutes. Brush out heavy runs and drips that don't penetrate.

Dense Surface Application Instructions
Apply in a single, saturating application with no run down. Back roll all runs and drips to ensure uniform appearance. DO NOT OVER APPLY. One application is normally enough. Always test.

Horizontal Application Instructions
1. Saturate in a single application. Use enough to keep the surface wet for 2 to 3 minutes before penetration.
2. Broom out puddles until they soak in. Treated surfaces dry to touch in 1 hour. Protect surfaces from rainfall for 6 hours following treatment. Many surfaces need several days to develop full water repellency.

Note: Protect from rain for 6 hours and from pedestrian and vehicular traffic until visibly dry.

Appendix F. EDS analysis report on mixed layer chlorite-smectite

Princeton Gamma-Tech, Inc.

Spectrum Report

Thursday, April 04, 2013

Live Time:	60.72	Count Rate:	879	Dead Time:	25.50 %
Beam Voltage:	28.91	Beam Current:	3.00	Takeoff Angle:	30.00

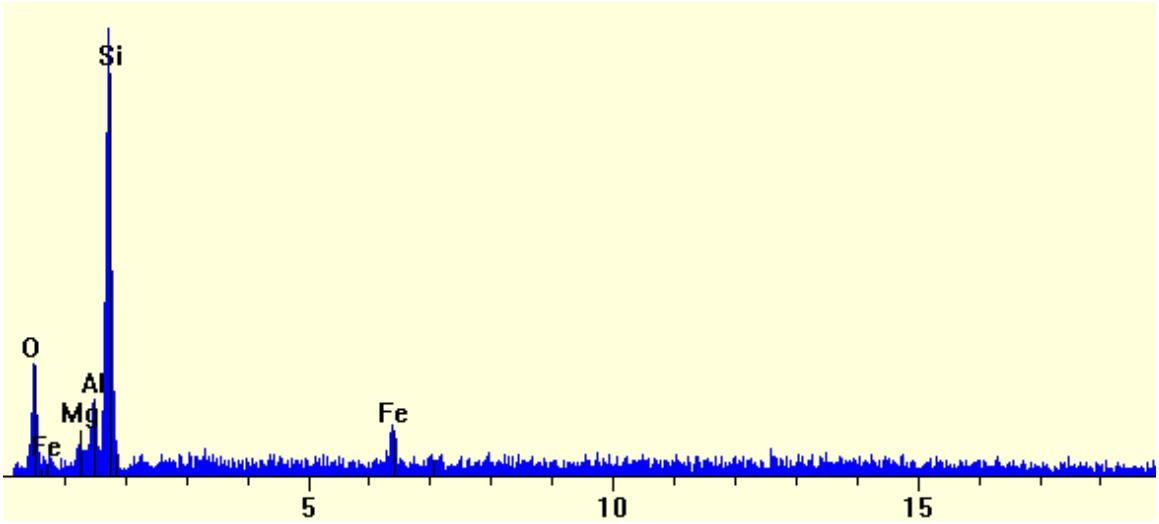

Element	Line	keV	KRatio	Wt%	At%	At Prop	ChiSquared
Fe	KA1	6.403	0.0648	7.71	3.17	0.0	0.98
Si	KA1	1.740	0.2705	48.32	39.51	0.0	5.80
Al	KA1	1.487	0.0393	7.50	6.39	0.0	5.80
O	KA1	0.523	0.0703	33.59	48.21	0.0	1.55
Mg	KA1	1.254	0.0124	2.87	2.71	0.0	5.80
Total			**0.4572**	**100.00**	**100.00**	**0.0**	**2.39**

Element	Line	Gross (cps)	BKG (cps)	Overlap (cps)	Net (cps)	P:B Ratio
Fe	KA1	18.6	5.5	0.0	13.1	2.4
Si	KA1	127.5	4.6	0.0	122.9	26.7
Al	KA1	22.7	4.4	0.0	18.2	4.1
O	KA1	26.2	2.6	0.0	23.6	9.1
Mg	KA1	10.1	4.2	0.0	5.9	1.4

Element	Line	Det Eff	Z Corr	A Corr	F Corr	Tot Corr	Modes
Fe	KA1	0.984	1.169	1.018	1.000	1.191	Element
Si	KA1	0.893	1.020	1.751	1.000	1.786	Element
Al	KA1	0.907	1.045	1.890	0.967	1.910	Element
O	KA1	0.516	0.939	5.098	0.999	4.780	Element
Mg	KA1	0.866	1.010	2.345	0.977	2.313	Element

Appendix G. Statistical Analysis Tools

G.1 Standard deviation from pooled data

In practical situations, where not that many measurements can be made on a given sample, the results of standard deviations obtained from different, but similar samples, measured with the same method, can be pooled to improve the experimental standard deviation *s,* provided that they pass the *F* test, described below. The pooled standard deviation obtained is a much better estimate than each individual *s.* The pooled standard deviation is calculated with the following equation:

$$s = \sqrt{\left[\sum (x_i - \bar{x}_1)^2 + \sum (x_i - \bar{x}_2)^2 + \cdots + \sum (x_i - x_k)^2\right] / (N - k)}$$

Where:
k = the number of samples (1 to k)
N = the sum of all measurements (N_1 to N_k)

G.2 Student *t* Test

The test serves, among other purposes, to compare the means of two sets of data. For this purpose the following experimental *t* is calculated as:

$$t = \left[\frac{x - y}{s}\right] \sqrt{MN/(M + N)}$$

Where:
x, y = the means of the two sets
s = the pooled standard deviation, and
M, N = the number of measurements within each set

If the calculated *t* is larger than the one listed in Table G.1 at the desired confidence level, there is a significant difference between the two means.

Table G.1 Values of t for ν degrees of freedom for various confidence levels.

Confidence Level / Degrees of Freedom ν	90%	95%	98%	99%	99.5%	99.8%	99.9%
1	6.314	12.71	31.82	63.66	127.3	318.3	636.6
2	2.920	4.303	6.965	9.925	14.09	22.33	31.60
3	2.353	3.182	4.541	5.841	7.453	10.21	12.92
4	2.132	2.776	3.747	4.604	5.598	7.173	8.610
5	2.015	2.571	3.365	4.032	4.773	5.893	6.869
6	1.943	2.447	3.143	3.707	4.317	5.208	5.959
7	1.895	2.365	2.998	3.499	4.029	4.785	5.408
8	1.860	2.306	2.896	3.355	3.833	4.501	5.041
9	1.833	2.262	2.821	3.250	3.690	4.297	4.781
10	1.812	2.228	2.764	3.169	3.581	4.144	4.587
15	1.753	2.131	2.602	2.947	3.286	3.733	4.073
20	1.725	2.086	2.528	2.845	3.153	3.552	3.850
25	1.708	2.060	2.485	2.787	3.078	3.450	3.725
∞	1.645	1.960	2.326	2.576	2.807	3.090	3.291

G.3 F Test

This test allows to estimate whether a significant difference exists in the precision of two sets of data. The ratio of the variances, ${s_1}^2$ and ${s_2}^2$ is calculated and compared to the critical values of *F* listed in tables as a function of the degrees of freedom of the numerator (the larger variance) and denominator as well as for a given confidence level.

$$F = {s_1}^2/{s_2}^2$$

If the calculated value is larger than the corresponding listed critical *F* there is a significant difference between the precision of the two methods. This test is also used to determine whether one population is more variable than another.

G.4 Analysis of Variance

This is used to determine whether significant differences exist among the means from different treatments. For this purpose the variation within and between the treatments has to be calculated.

G.4.1 Variance within treatments:

The sum of the Squares S for each sample is calculated as:

$$S_1 = \sum (x_{i_1} - \bar{x}_1)^2$$
$$S_2 = \sum (x_{i_2} - \bar{x}_2)^2$$
$$\dots$$

Then the overall sum of squares for within treatments is calculated as:

$$S_R = S_1 + S_2 + \cdots + S_k$$

Where k = the number of treatments

The corresponding variance or within-treatment mean square is calculated as:

$$s_R{}^2 = S_R/\nu_R$$

Where:
ν_R = N – k degrees of freedom
N = total number of measurements

G.4.2 Variance between treatments:

All the data are pooled, and the grand average $\bar{x}$ is calculated. The between treatment sum of squares is calculated as:

$$S_T = n_1(\bar{x}_1 - \bar{x})^2 + n_2(\bar{x}_2 - \bar{x})^2 + \cdots + n_k(\bar{x}_k - \bar{x})^2$$

Where:
k = number of treatments
n = number of data points in each treatment
The variance or between-treatment mean square is calculated as:

$$s_T{}^2 = S_T/\nu_T$$

Where ν_T = k – 1 degrees of freedom

G.4.3 Summary

To summarize the results, the following table is constructed:

	Sum of Squares	Degrees of Freedom	Mean Squares
Between Treatment	s_T	$\boldsymbol{\nu}_T$	${s_T}^2$
Within Treatment	s_R	$\boldsymbol{\nu}_R$	${s_R}^2$
Ratio of Mean Squares	${s_T}^2/{s_R}^2$		

If the difference between the two mean squares is large it can be supposed that there is a significant difference between the treatments. The ratio of the mean squares can be calculated and compared to the critical *F* values listed at the selected confidence level (note that in the table $\boldsymbol{\nu}_1 = \boldsymbol{\nu}_T$ and $\boldsymbol{\nu}_2 = \boldsymbol{\nu}_R$). If ${s_T}^2/{s_R}^2 > F$, there is a significant difference between the treatments at that confidence level.

Table G.2 Values of F at 95 % confidence level

ν_1 / ν_2	1	2	3	4	5	6	7	8	9	10
1	161.45	199.50	215.71	224.58	230.16	233.99	236.77	238.88	240.54	241.88
2	18.51	19.00	19.16	19.25	19.30	19.33	19.35	19.37	19.38	19.40
3	10.13	9.55	9.28	9.12	9.01	8.94	8.89	8.85	8.81	8.79
4	7.71	6.94	6.59	6.39	6.26	6.16	6.09	6.04	6.00	5.96
5	6.61	5.79	5.41	5.19	5.05	4.95	4.88	4.82	4.77	4.74
6	5.99	5.14	4.76	4.53	4.39	4.28	4.21	4.15	4.10	4.06
7	5.59	4.74	4.35	4.12	3.97	3.87	3.79	3.73	3.68	3.64
8	5.32	4.46	4.07	3.84	3.69	3.58	3.50	3.44	3.39	3.35
9	5.12	4.26	3.86	3.63	3.48	3.37	3.29	3.23	3.18	3.14
10	4.96	4.10	3.71	3.48	3.33	3.22	3.14	3.07	3.02	2.98
13	4.67	3.81	3.41	3.18	3.03	2.92	2.83	2.77	2.71	2.67
15	4.54	3.68	3.29	3.06	2.90	2.79	2.71	2.64	2.59	2.54

Index